SUPPORTING INFORMATION

Hexadecyl-containing organic salts as novel organogelators for ionic, eutectic, and molecular liquids

Cesar N. Prieto Kullmer,[a] Daniel Ta,[a] Christian Y. Chen,[a] Christopher J. Cieker,[a] Onofrio Annunziata[a] and Sergei V. Dzyuba[a]*

[a] Department of Chemistry and Biochemistry, Texas Christian University, Fort Worth, TX 76129, USA

FOR TABLE OF CONTENTS ONLY

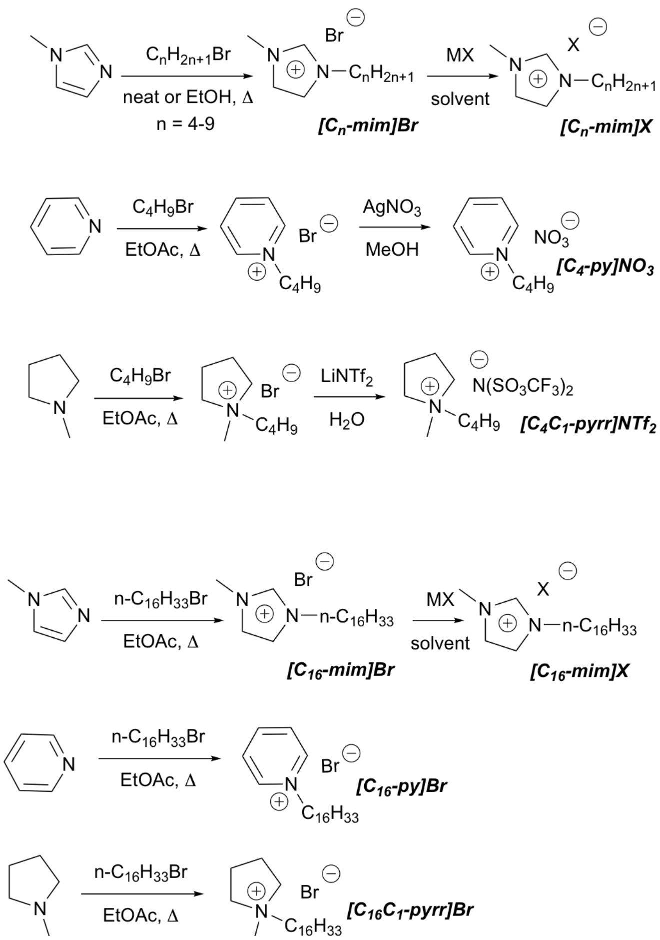

X	M	solvent
PF_6	K	H_2O
BF_4	Na	CH_3CN
NO_3	Ag	MeOH
TFA	Ag	MeOH
NTf_2	Li	H_2O

X	M	solvent
PF_6	K	H_2O
BF_4	Ag	MeOH
TFA	Ag	MeOH
NTf_2	Li	H_2O

Scheme S1. Syntheses of ionic liquids and gelators.

NMR description of ionic liquids and gelators

[C_4-mim]Br:[1]

^{1}H NMR (400 MHz, $CDCl_3$): δ = 10.29 (s, 1H), 7.54 (t, *J* = 1.7 Hz, 1H), 7.43 (t, *J* = 1.7Hz, 1H), 4.35 (t, *J* = 7.2 Hz, 2H), 4.13 (s, 3H), 1.91 (pent, *J* = 7.4 Hz, 2H), 1.39 (sext, *J* = 7.2 Hz, 2H), 0.97 (t, *J* = 7.6 Hz, 3H).

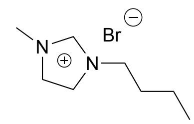

[C_5-mim]Br:[1]

^{1}H NMR (400 MHz, $CDCl_3$): δ = 10.60 (s, 1H), 7.37 (s,1H), 7.29 (s, 1H), 4.33 (t, *J* = 7.2 Hz, 2H), 4.14 (s, 3H), 1.93 (pent, *J* = 7.6 Hz, 2H), 1.37 (m, 4H), 0.91 (t, *J* = 6.8 Hz, 3H).

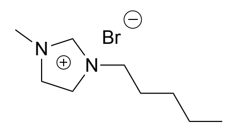

[C_6-mim]Br:[1]

^{1}H NMR (400 MHz, $CDCl_3$): δ = 10.65 (s, 1H), 7.32 (s,1H), 7.25 (s, 1H), 4.33 (t, *J* = 7.4 Hz, 2H), 4.13 (s, 3H), 1.93 (pent, *J* = 7.5 Hz, 2H), 1.36 (m, 6H), 0.89 (t, *J* = 7.0 Hz, 3H).

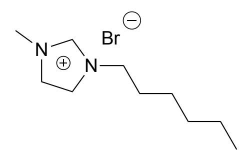

[C_7-mim]Br:[1]

^{1}H NMR (400 MHz, $CDCl_3$): δ = 10.52 (s, 1H), 7.38 (m, 1H), 7.43 (m, 1H), 4.32 (t, *J* = 7.4 Hz, 2H), 4.11 (s, 3H), 1.92 (pent, *J* = 7.3 Hz, 2H), 1.32 (m, 8H), 0.88 (t, *J* = 6.9 Hz, 3H).

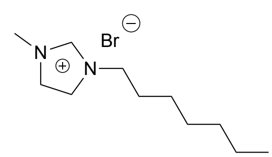

[C_8-mim]Br:[1]

^{1}H NMR (400 MHz, $CDCl_3$): δ = 10.74 (s, 1H), 7.25 (s, 1H), 7.20 (s, 1H), 4.32 (t, *J* = 7.4 Hz, 2H), 4.13 (s, 3H), 1.92 (pent, *J* = 7.3 Hz, 2H), 1.31 (m, 10H), 0.88 (t, *J* = 6.7 Hz, 3H).

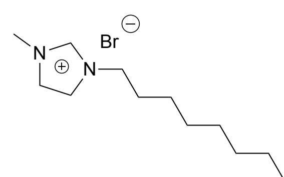

[C_9-mim]Br:[1]

^{1}H NMR (400 MHz, $CDCl_3$): δ = 10.75 (s, 1H), 7.25 (m, 1H), 7.20 (m, 1H), 4.32 (t, *J* = Hz, 2H), 4.13 (s, 3H), 1.92 (pent, *J* = 7.2 Hz, 2H), 1.34 (m, 12H), 0.88 (t, *J* = 6.8 Hz, 3H).

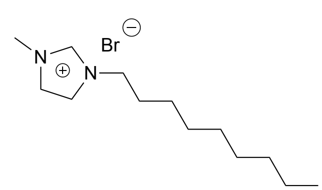

[C_4-mim]PF_6:[2]

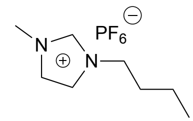

^{1}H NMR (400 MHz, acetone-d$_6$): δ = 9.02 (s, 1H), 7.79 (t, *J* = 1.7 Hz, 1H), 7.73 (t, *J* = 1.7 Hz, 1H), 4.39 (t, *J* = 7.2 Hz, 2H), 4.08 (s, 3H), 1.75 (pent, *J* = 7.5 Hz, 2H), 1.24 (sext, *J* = 7.5 Hz, 2H), 0.96 (t, *J* = 7.3 Hz, 3H);
^{19}F NMR (376 MHz, acetone-d$_6$): δ = –70.2 (d, *J* = 710 Hz);
^{31}P (162 Hz, acetone-d$_6$): δ = –144.3 (sept, *J* = 708 Hz).

[C_6-mim]PF_6:[2]

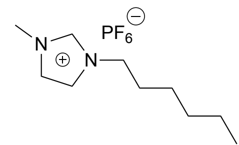

^{1}H NMR (400 MHz, acetone-d$_6$): δ = 8.95 (s, 1H), 7.71 (t, *J* = 1.8 Hz, 1H), 7.65 (t, *J* = 1.8 Hz, 1H), 4.33 (t, *J* = 7.3 Hz, 2H), 4.02 (s, 3H), 1.93 (pent, *J* = 7.5 Hz, 2H), 1.33 (m, 6H), 0.88 (t, *J* = 7.1 Hz, 3H);
^{19}F NMR (376 MHz, acetone-d$_6$): δ = –72.2 (d, *J* = 708 Hz);
^{31}P (162 Hz, acetone-d$_6$): δ = –144.3 (sept, *J* = 708 Hz).

[C_4-mim]NO_3:[3]

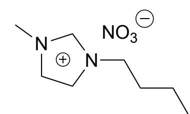

^{1}H NMR (400 MHz, DMSO-d$_6$): δ = 9.19 (s, 1H), 7.79 (t, *J* = 1.7 Hz, 1H), 7.72 (t, *J* = 1.7 Hz, 1H), 4.17 (t, *J* = 7.1 Hz, 2H), 3.86 (s, 3H), 1.76 (pent, *J* = 7.2 Hz, 2H), 1.27 (sext, *J* = 7.4 Hz, 2H), 0.90 (t, *J* = 7.3 Hz, 3H).

[C_6-mim]NO_3:[3]

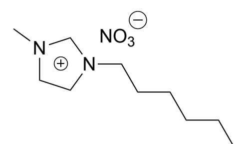

^{1}H NMR (400 MHz, DMSO-d$_6$): δ = 9.14 (s, 1H), 7.79 (t, *J* = 1.7 Hz, 1H), 7.72 (t, *J* = 1.7 Hz, 1H), 4.16 (t, *J* = 7.2 Hz, 2H), 3.86 (s, 3H), 1.78 (pent, *J* = 7.0 Hz, 2H), 1.27 (m, 6H), 0.87 (t, *J* = 7.1 Hz, 3H).

[C_4-mim]NTf_2 or **C_4-mim]$N(SO_2CF_3)_2$**:[2]

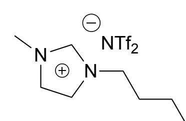

^{1}H NMR (400 MHz, DMSO-d$_6$): δ = 9.11 (s, 1H), 7.76 (t, *J* = 1.7 Hz, 1H), 7.70 (t, *J* = 1.8 Hz, 1H), 4.17 (t, *J* = 7.1 Hz, 2H), 3.86 (s, 3H), 1.77 (pent, *J* = 7.3 Hz, 2H), 1.27 (sext, *J* = 7.4 Hz, 2H), 0.93 (t, *J* = 7.3 Hz, 3H);
^{19}F NMR (376 MHz, DMSO-d$_6$): δ = –78.8 (s).

[C_6-mim]NTf_2 or **[C_6-mim]$N(SO_2CF_3)_2$**:[2]

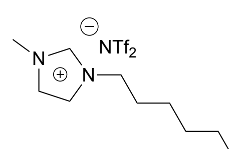

^{1}H NMR (400 MHz, acetone-d$_6$): δ = 9.32 (s, 1H), 7.81 (t, *J* = 1.7 Hz, 1H), 7.74 (t, *J* = 1.7 Hz, 1H), 4.38 (t, *J* = 7.3 Hz, 2H), 4.08 (s, 3H), 1.95 (pent, *J* = 7.3 Hz, 2H), 1.37 (m, 6H), 0.86 (t, *J* = 7.1 Hz, 3H);
^{19}F NMR (376 MHz, DMSO-d$_6$): δ = –79.9 (s).

[C_4-mim]BF_4:[4]

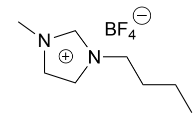

^{1}H NMR (400 MHz, acetone-d_6): δ = 9.96 (s, 1H), 7.99 (t, *J* = 1.8 Hz, 1H), 7.91 (t, *J* = 1.8 Hz, 1H), 4.46 (t, *J* = 7.2 Hz, 2H), 4.11 (s, 3H), 1.92 (m, 2H), 1.37 (sext, *J* = 7.5 Hz, 2H), 0.94 (t, *J* = 7.4 Hz, 3H);
^{19}F (376 MHz, acetone-d_6): δ = –150.9 (m).

[C_4-mim]TFA or **[C_4-mim]CF_3CO_2:**[5]

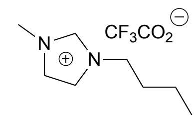

^{1}H NMR (400 MHz, DMSO-d_6): δ = 9.17 (s, 1H), 7.79 (t *J* = 1.7 Hz, 1H), 7.72 (t, *J* = 1.7 Hz, 1H), 4.17 (t, *J* = 7.1 Hz, 2H), 3.85 (s, 3H), 1.77 (m, 2H), 1.28 (sext, *J* = 7.4 Hz, 2H), 0.91 (t, *J* = 7.3 Hz, 3H);
^{19}F (376 MHz, DMSO-d_6): δ = –73.4 (s).

[C_4-py]NO_3:[3]

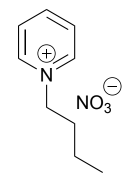

^{1}H NMR (400 MHz, acetone-d_6): δ = 9.46 (d, *J* = 5.6 Hz, 2H), 8.75 (t, *J* = 8.8 Hz, 1H), 8.28 (d, *J* = 6.9 Hz, 2H), 4.91 (t, *J* = 6.5 Hz, 2H), 2,07 (m, 2H), 1.43 (sext, *J* = 7.4 Hz, 2H), 0.98 (t, *J* = 7.3 Hz, 3H).

[C_4C_1-pyrr]NTf_2 [C_4C_1-pyrr]$N(SO_2CF_3)_2$:[6]

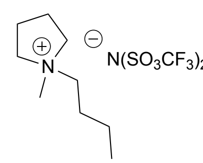

^{1}H NMR (400 MHz, DMSO-d_6): δ = 3.42 (m, 4H), 3.00 (m, 2H), 2.98 (s, 3H), 2.08 (m, 4H), 1.68 (m, 4H), 1.33 (sext, *J* = 7.5 Hz, 2H), 0.94 (t, *J* = 7.5 Hz, 3H);
^{19}F (376 MHz, DMSO-d_6): δ = –78.8 (s).

[C_{16}-mim]Br:[7]

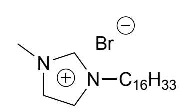

^{1}H NMR (400 MHz, acetone-d_6): δ = 10.19 (m, 1H), 7.86 (m, 1H), 7.80 (m, 1H), 4.43 (t, *J* = 7.2 Hz, 2H), 4.09 (s, 3H), 1.96 (pent, *J* = 7.2 Hz, 2H), 1.30 (m, 26H), 0.87 (t, *J* = 6.5 Hz, 3H).

[C_{16}-mim]BF_4:[4]

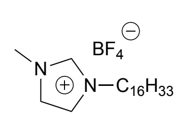

^{1}H NMR (400 MHz, acetone-d_6): δ = 9.02 (m, 1H), 7.77 (m, 1H), 7.72 (m, 1H), 4.37 (m, 2H), 4.06 (m, 3H), 1.96 (m, 2H), 1.33 (m, 26H), 0.87 (t, *J* = 6.7 Hz, 3H);
^{19}F (376 MHz, acetone-d_6): δ = –151.1 (m).

[C_{16}-mim]PF_6:[8]

[1]H NMR (400 MHz, acetone-d_6): δ = 9.08 (m, 1H), 7.80 (m, 1H), 7.74 (m, 1H), 4.39 (t, *J* = 7.5 Hz, 2H), 4.09 (s, 3H), 1.97 (pent, *J* = 7,1 Hz, 2H), 1.34 (m, 26H), 0.86 (t, *J* = 7.0 Hz, 3H).
[19]F (376 MHz, acetone-d_6): δ = –72.5 (d, *J* = 708 Hz);
[31]P (162 Hz, acetone-d_6): δ = –144.3 (sept, *J* = 708 Hz).

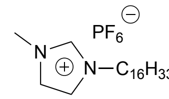

[C_{16}-mim]TFA or **[C_{16}-mim]CF_3CO_2**:

[1]H NMR (400 MHz, acetone-d_6): δ = 9.86 (m, 1H), 7.80 (m, 1H), 7.74 (m, 1H), 4.37 (t, *J* = 7.3 Hz, 2H), 4.06 (s, 3H), 2.97 (m, 2H), 1.30 (m, 26H), 0.86 (m, 3H);
[19]F (376 MHz, acetone-d_6): δ = –79.9 (m).

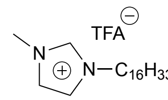

[C_{16}-mim]NTf_2 or **[C_{16}-mim]$N(SO_2CF_3)_2$**:[9]

[1]H NMR (400 MHz, acetone-d_6): δ = 9.08 (m, 1H), 7.80 (m, 1H), 7.74 (m, 1H), 4.38 (m, 2H), 4.08 (m, 3H), 1.94 (m, 2H), 1.30 (m, 26H), 0.87 (t, *J* = 6.6 Hz, 3H);
[19]F (376 MHz, acetone-d_6): δ = –75.0 (m).

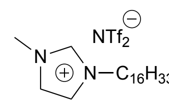

[C_{16}-py]Br:[10]

[1]H NMR (400 MHz, $CDCl_3$): δ = 9.45 (d, *J* = 6.0 Hz, 2H), 8.50 (t, *J* = 7.9 Hz, 1H), 8.12 (t, *J* = 6.8 Hz, 2H), 5.03 (t, *J* = 6.7 Hz, 2H), 2.04 (pent, *J* = 7.2 Hz, 2H), 1.70 (m, 4H), 1.30 (m, 24H), 0.88 (t, *J* = 6.4 Hz, 3H).

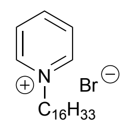

[$C_{16}C_1$-pyrr]Br:[11]

[1]H NMR (400 MHz, $CDCl_3$): δ = 3.83 (m, 4H), 3.65 (m, 2H), 2,31 (m, 4H), 1.74 (m, 4H), 1.20 (m, 24H), 0.88 (t, *J* = 6.8 Hz, 3H).

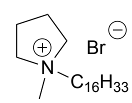

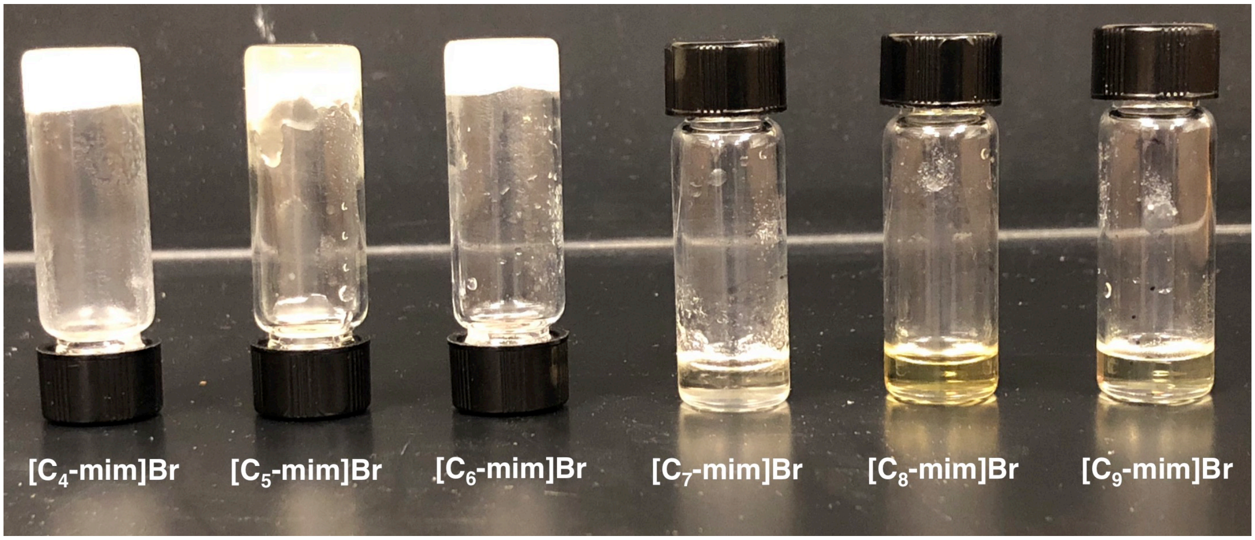

Figure S1. Photographs of [C_n-mim]Br ionic liquids (0.5 ml) in the presence of [C_{16}-mim]Br. n = 4 –9; [C_{16}-mim]Br = 10.0 % w/v.

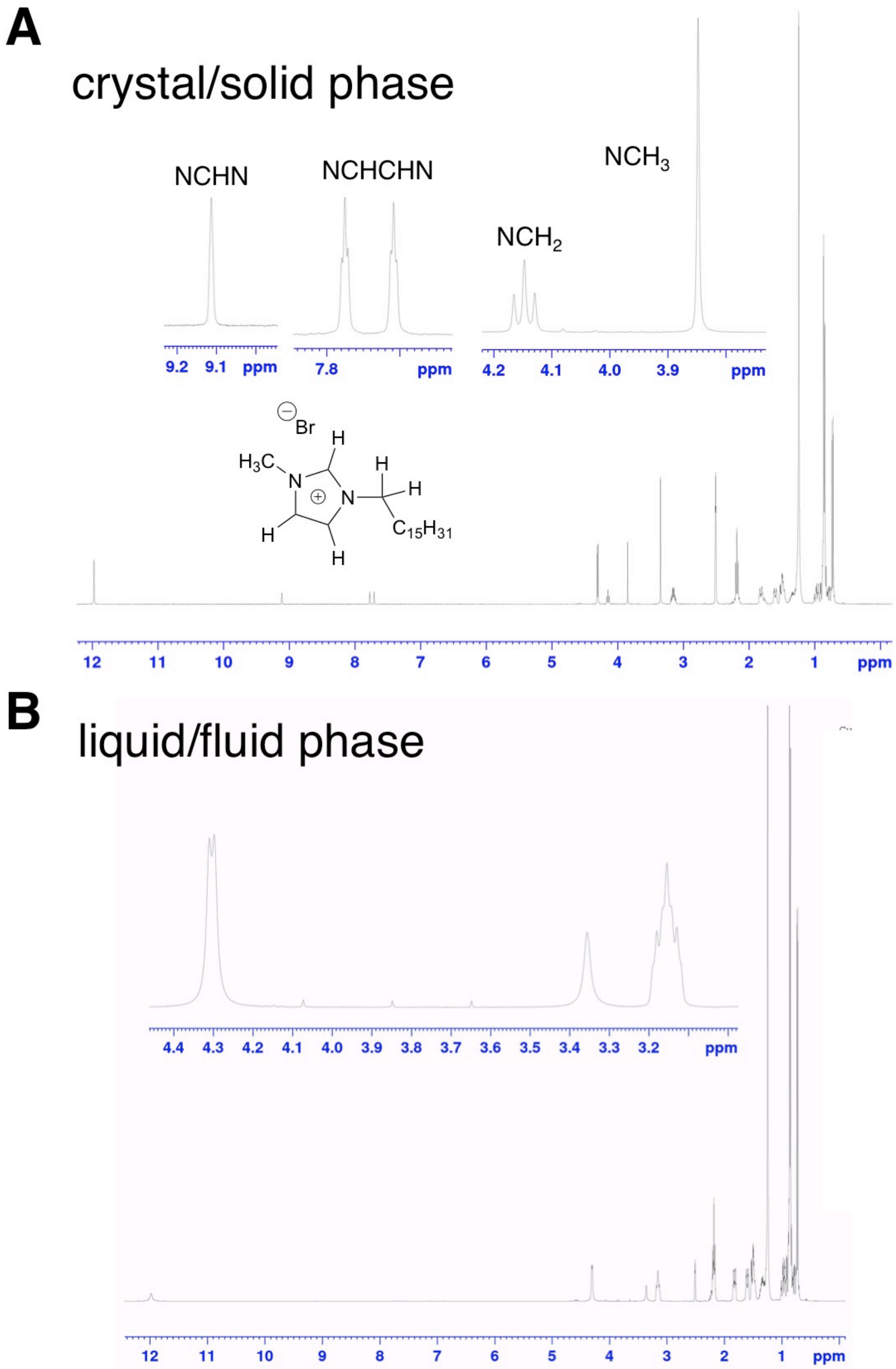

Figure S2. [1]H NMR of the deconstructed L-ment/$C_{11}H_{23}CO_2H$–[C_{16}-mim]Br gel.
The gel was centrifuged to separate the liquid and solid components. The liquid component was pipetted out and the remaining solid component was pressed to release the residual fluid. **A**: crystal/solid phase that contains [C_{16}-mim]Br; the expanded regions show the H-resonances for the protons of the imidazolium ring CH_3 and CH_2 groups on the nitrogens of the imidazolium ring. **B**: fluid/liquid phase that does not contain [C_{16}-mim]Br; the expanded region highlights the absence of CH_3 and CH_2 resonances; in addition, no signals are observed in 10–7 ppm region).

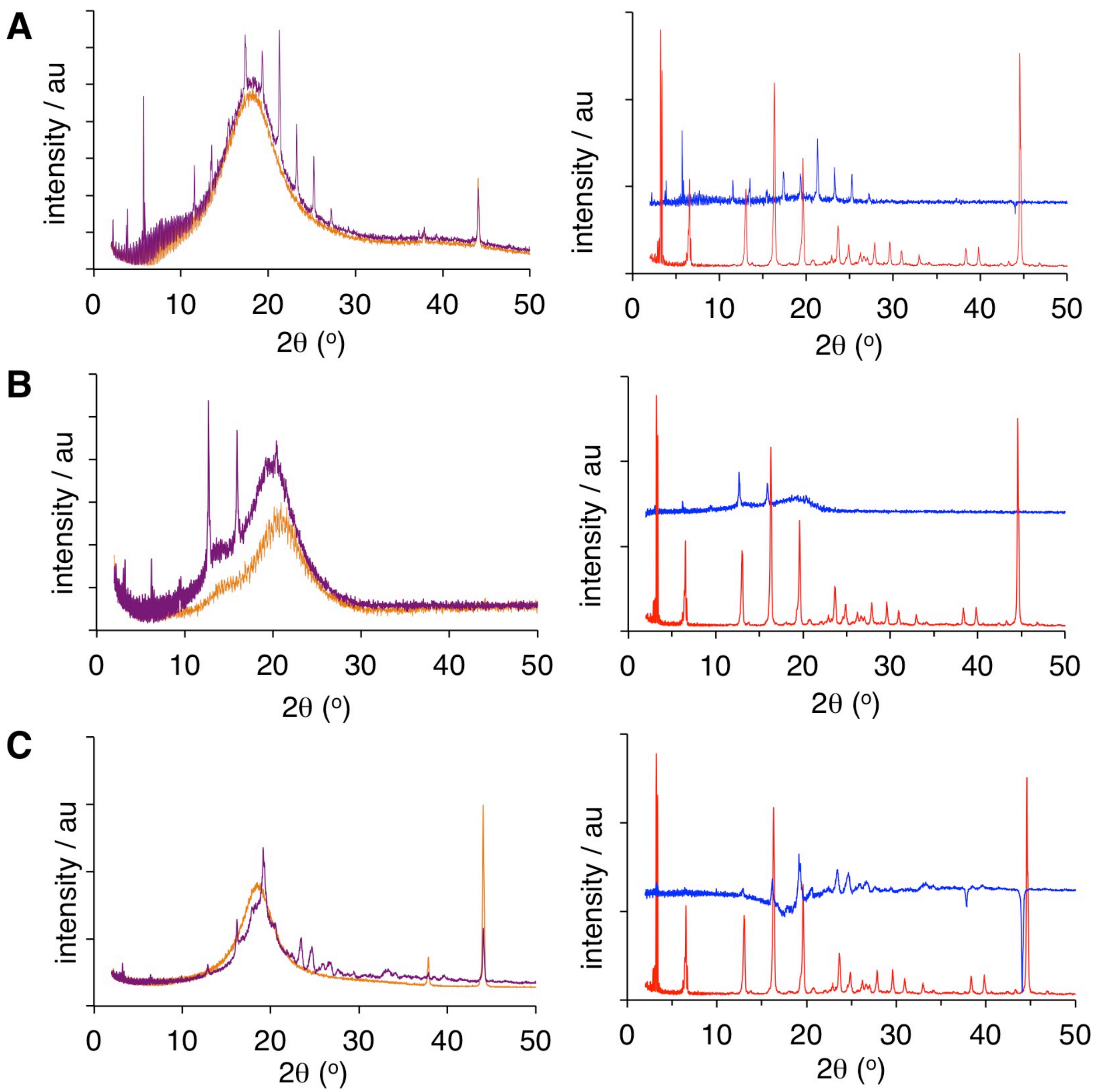

Figure S3. Powder XRD of the gels and the neat gelator.

A: left: L-menth/$C_{11}H_{23}CO_2H$ gel, 0.9% w/v [C_{16}-mim]Br (purple) and L-menth/$C_{11}H_{23}CO_2H$ (organge); right: L-menth/$C_{11}H_{23}CO_2H$ gel, 0.9% w/v [C_{16}-mim]Br (blue, with L-menth/$C_{11}H_{23}CO_2H$ pattern subtracted), and [C_{16}-mim]Br (red); the x-ray patterns are artificially off-set.

B: left: [C_4-mim]PF_6 gel, 6.0% w/v [C_{16}-mim]Br (purple) and [C_4-mim]PF_6 (orange); right: [C_4-mim]PF_6 gel, 6.0% w/v [C_{16}-mim]Br (blue, with [C_4-mim]PF_6 pattern subtracted), and [C_{16}-mim]Br (red); the x-ray patterns are artificially off-set.

C: left: dioxane gel, 9.9% w/v [C_{16}-mim]Br (purple) and dioxane (orange); right: dioxane gel, 9.9% w/v [C_{16}-mim]Br (blue, with dioxane pattern subtracted), and [C_{16}-mim]Br (red); the x-ray patterns are artificially off-set. Dioxane evaporated during the measurements.

Measurements were taken at room temperature.

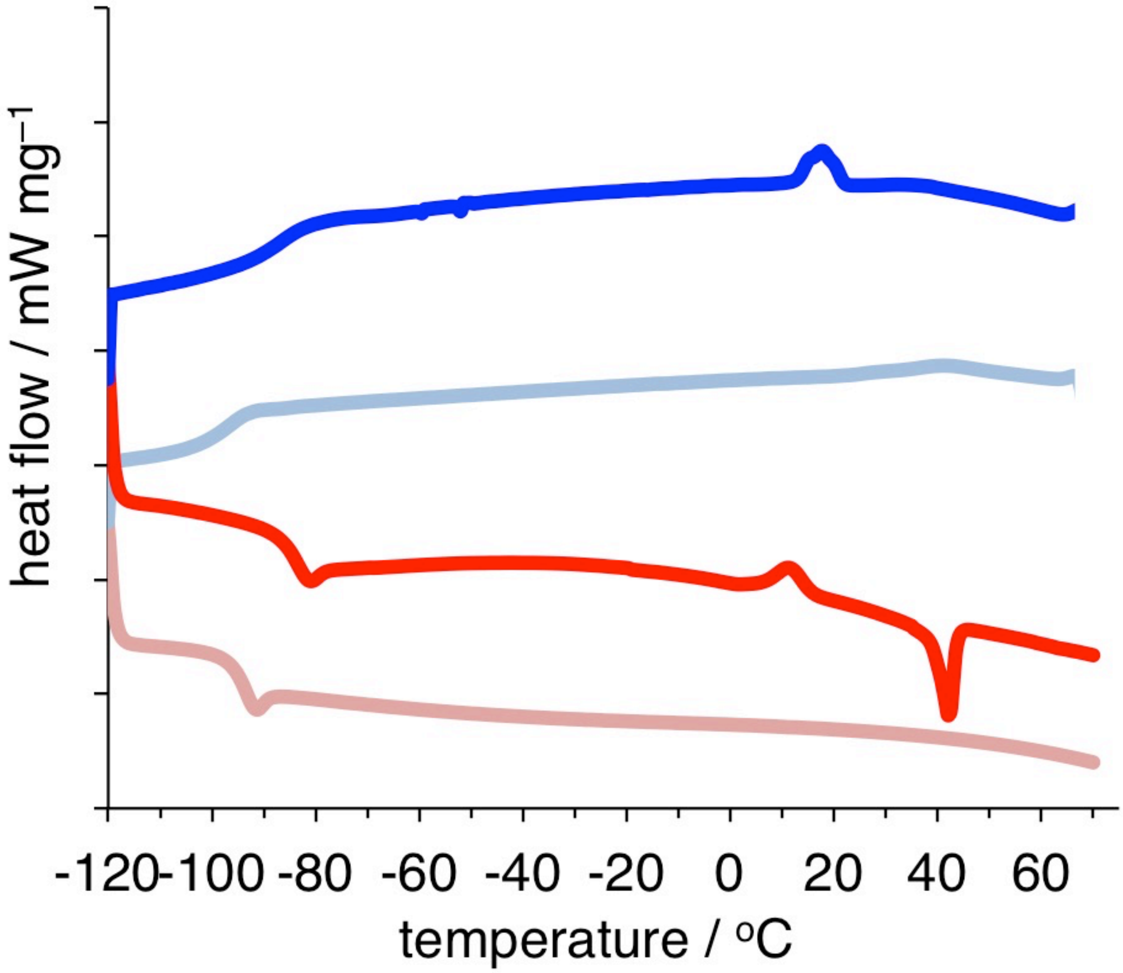

Figure S4. DSC traces of [C_4-mim]Br and [C_4-mim]Br–[C_{16}-mim]Br gel.
Conditions: samples were heated from 25 ^{o}C to 70 ^{o}C (not shown), cooling from 70 ^{o}C to –120 ^{o}C (blue traces), heating from –120 ^{o}C to 70 ^{o}C (red traces). The traces were artificially off-set to demonstrate the differences. [C_{16}-mim]Br concentration was 5.1 % w/v.

[C_4-mim]Br ionic liquid: pale blue (cooling) and pale red (heating);
[C_4-mim]Br–[C_{16}-mim]Br gel: bright blue (cooling) and bright red (heating).

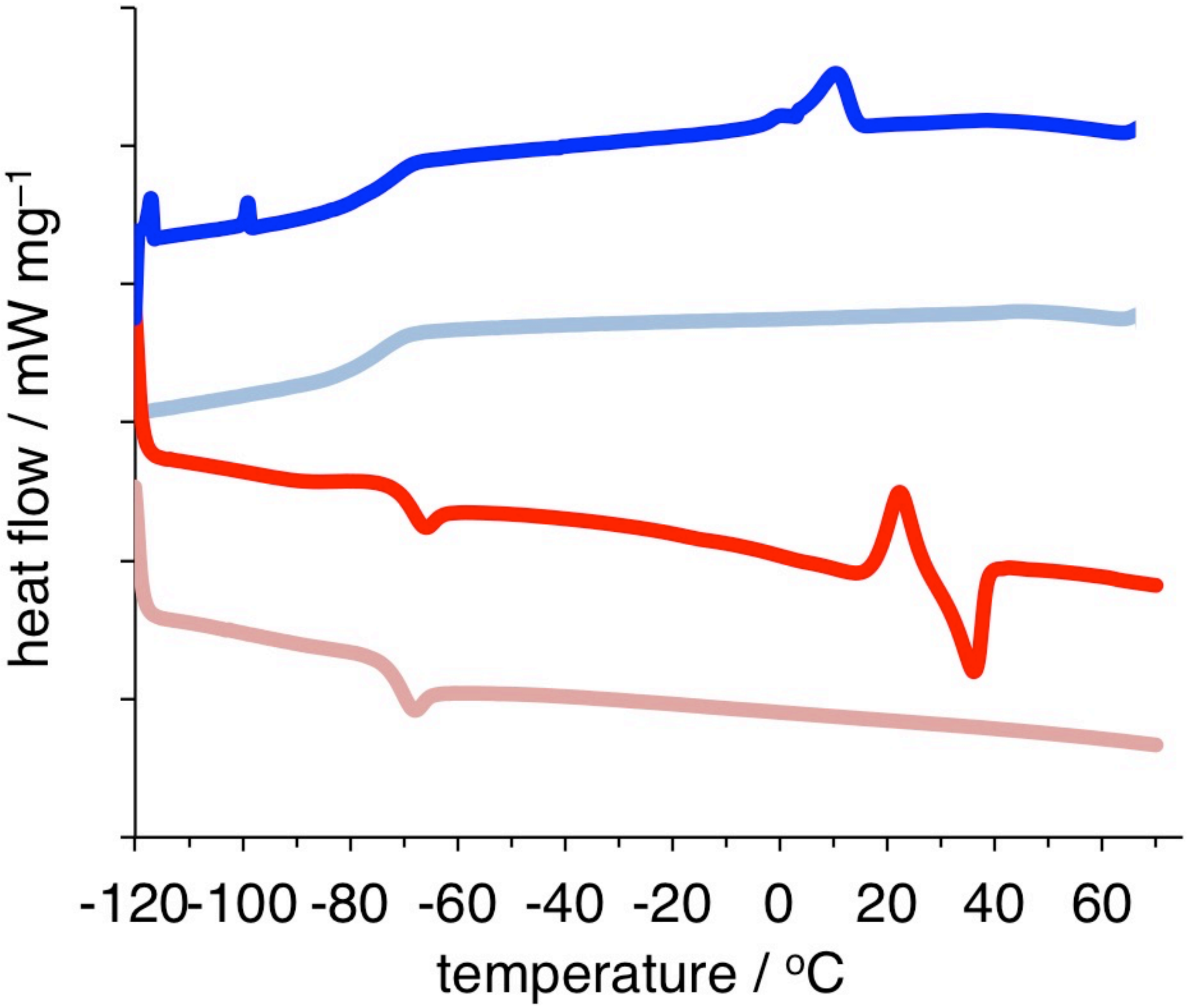

Figure S5. DSC traces of [C_5-mim]Br and [C_4-mim]Br–[C_{16}-mim]Br gel.
Conditions: samples were heated from 25 ^{o}C to 70 ^{o}C (not shown), cooling from 70 ^{o}C to –120 ^{o}C (blue traces), heating from –120 ^{o}C to 70 ^{o}C (red traces). The traces were artificially off-set to demonstrate the differences. [C_{16}-mim]Br concentration was 10.0 % w/v.

[C_5-mim]Br ionic liquid: pale blue (cooling) and pale red (heating);
[C_5-mim]Br–[C_{16}-mim]Br gel: bright blue (cooling) and bright red (heating).

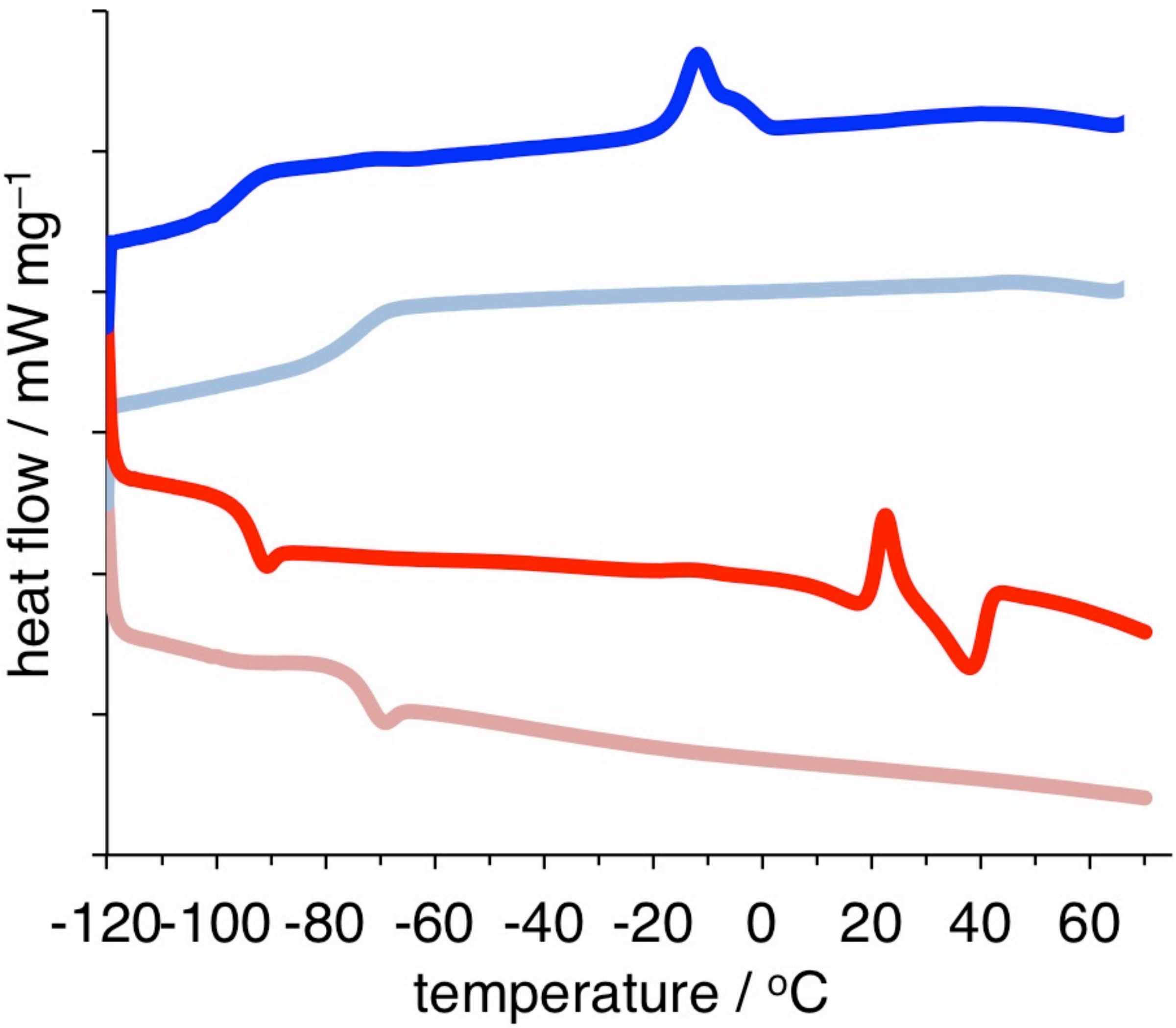

Figure S6. DSC traces of [C_6-mim]Br and [C_6-mim]Br–[C_{16}-mim]Br gel.
Conditions: samples were heated from 25 °C to 70 °C (not shown), cooling from 70 °C to –120 °C (blue traces), heating from –120 °C to 70 °C (red traces). The traces were artificially off-set to demonstrate the differences. [C_{16}-mim]Br concentration was 10.0 % w/v.

[C_6-mim]Br ionic liquid: pale blue (cooling) and pale red (heating);
[C_6-mim]Br–[C_{16}-mim]Br gel: bright blue (cooling) and bright red (heating).

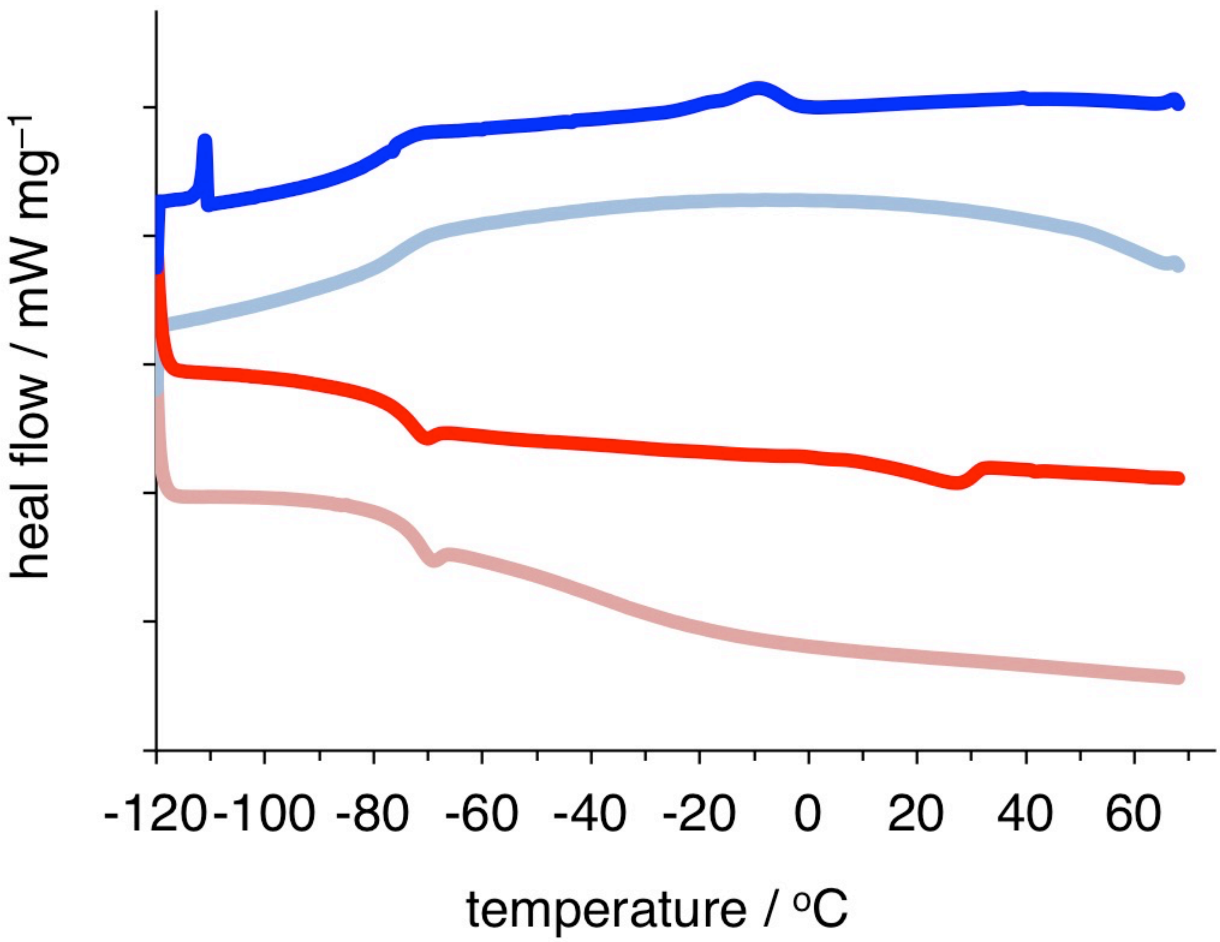

Figure S7. DSC traces of [C_6-mim]PF_6 and [C_6-mim]PF_6–[C_{16}-mim]Br gel.
Conditions: samples were heated from 25 ^{o}C to 70 ^{o}C (not shown), cooling from 70 ^{o}C to –120 ^{o}C (blue traces), heating from –120 ^{o}C to 70 ^{o}C (red traces). The traces were artificially off-set to demonstrate the differences. [C_{16}-mim]Br concentration was 5.0 % w/v.

[C_6-mim]PF_6 ionic liquid: pale blue (cooling) and pale red (heating);
[C_6-mim]PF_6–[C_{16}-mim]Br gel: bright blue (cooling) and bright red (heating).

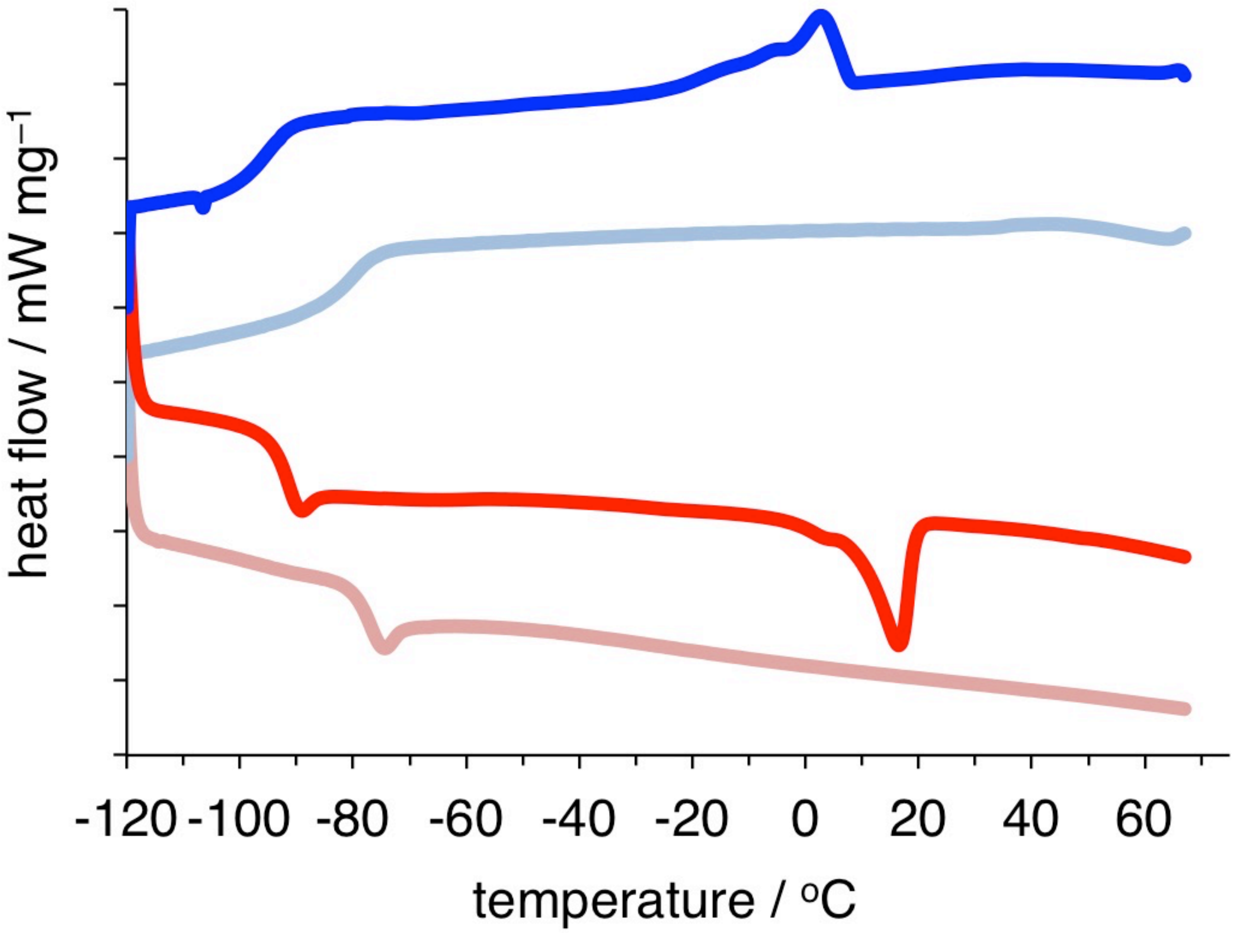

Figure S8. DSC traces of [C_6-mim]NO_3 and [C_6-mim]NO_3–[C_{16}-mim]Br gel.
Conditions: samples were heated from 25 ^{o}C to 70 ^{o}C (not shown), cooling from 70 ^{o}C to –120 ^{o}C (blue traces), heating from –120 ^{o}C to 70 ^{o}C (red traces). The traces were artificially off-set to demonstrate the differences. [C_{16}-mim]Br concentration was 11.0 % w/v.

[C_6-mim]NO_3 ionic liquid: pale blue (cooling) and pale red (heating);
[C_6-mim]NO_3–[C_{16}-mim]Br gel: bright blue (cooling) and bright red (heating).

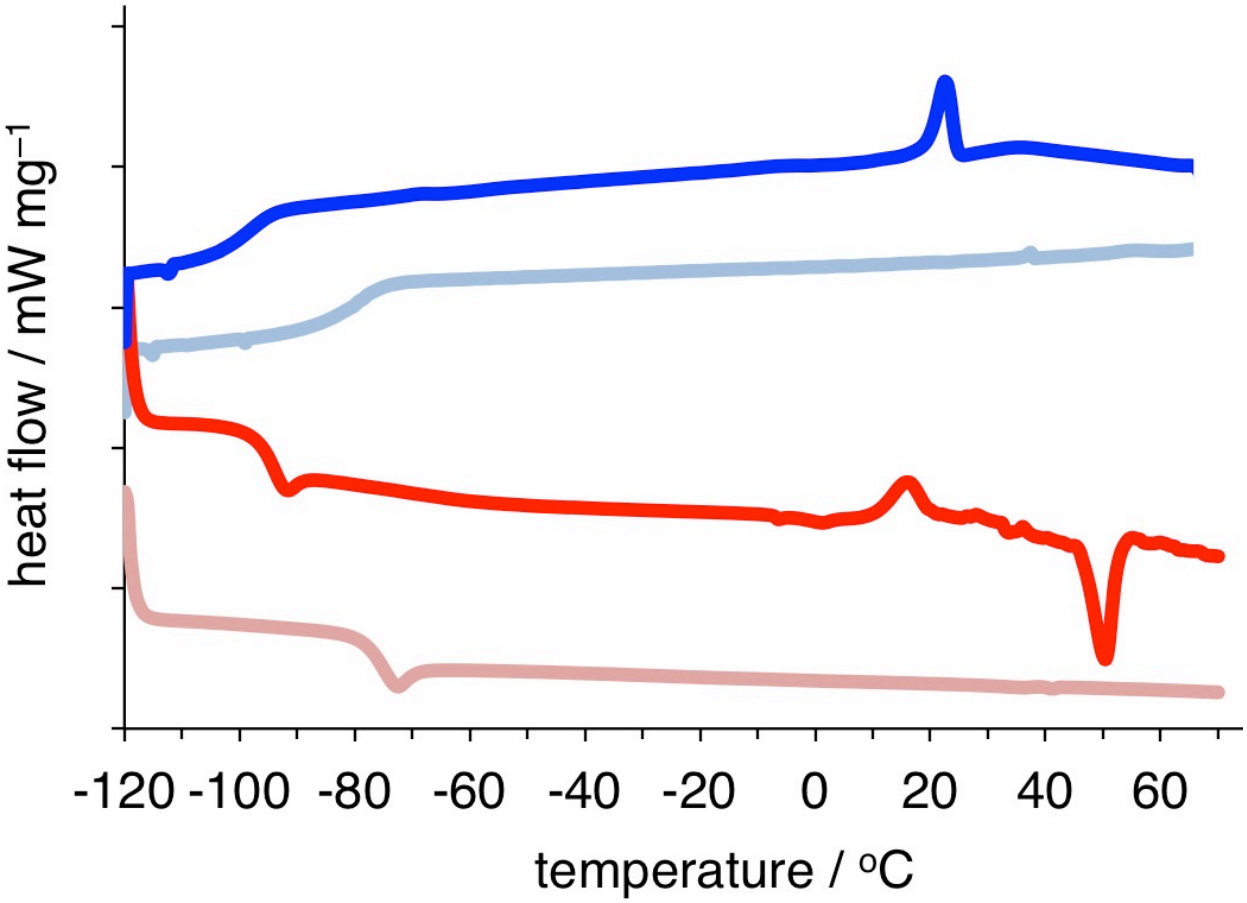

Figure S9. DSC traces of [C_4-mim]BF_4 and [C_4-mim]BF_4–[C_{16}-mim]Br gel.
Conditions: samples were heated from 25 ^{o}C to 70 ^{o}C (not shown), cooling from 70 ^{o}C to –120 ^{o}C (blue traces), heating from –120 ^{o}C to 70 ^{o}C (red traces). The traces were artificially off-set to demonstrate the differences. [C_{16}-mim]Br concentration was 5.5 % w/v.

[C_4-mim]BF_4 ionic liquid: pale blue (cooling) and pale red (heating);
[C_4-mim]BF_4–[C_{16}-mim]Br gel: bright blue (cooling) and bright red (heating).

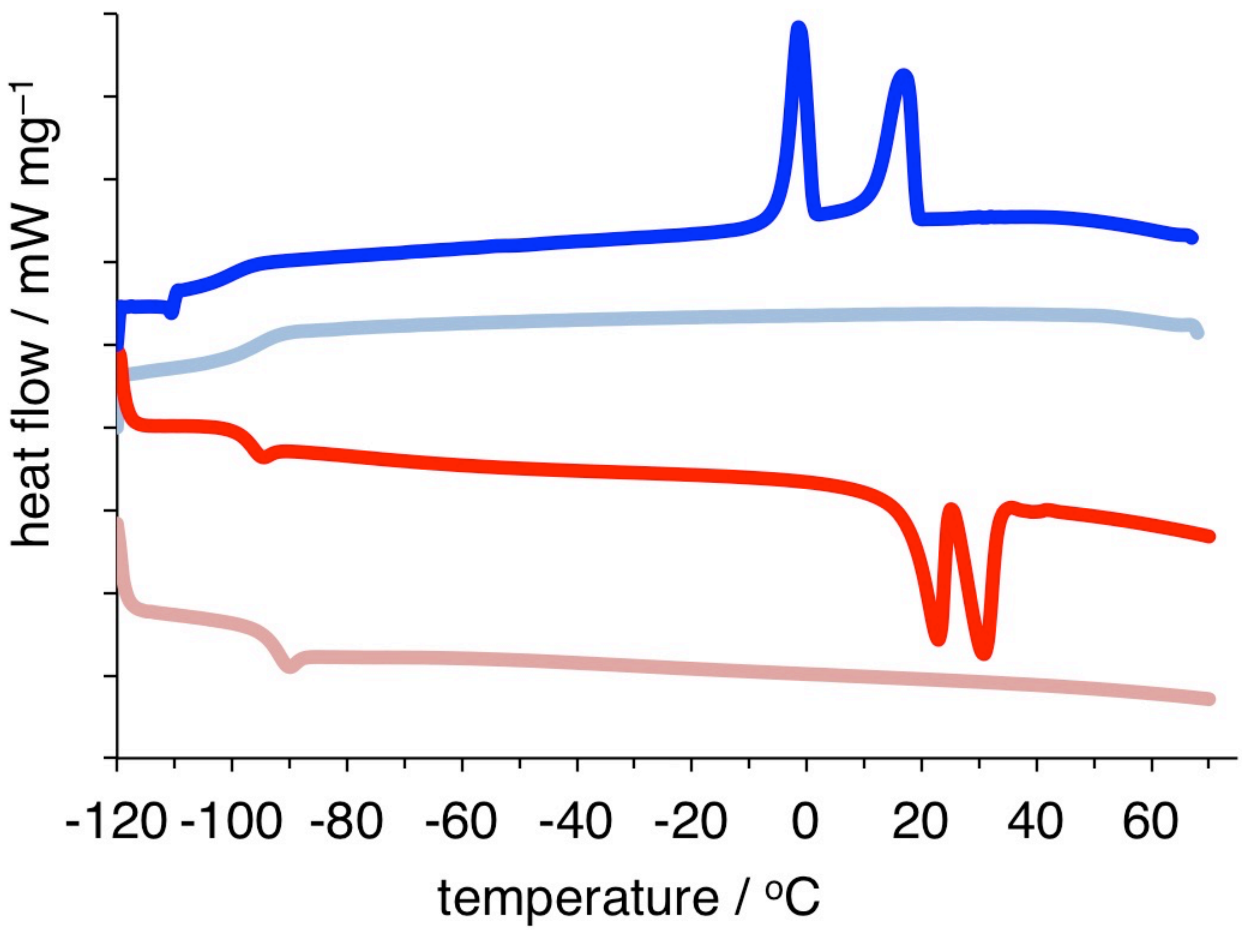

Figure S10. DSC traces of [C_4-mim]TFA and [C_4-mim]TFA–[C_{16}-mim]Br solution. Conditions: samples were heated from 25 ^{o}C to 70 ^{o}C (not shown), cooling from 70 ^{o}C to –120 ^{o}C (blue traces), heating from –120 ^{o}C to 70 ^{o}C (red traces). The traces were artificially off-set to demonstrate the differences. [C_{16}-mim]Br concentration was 21.6 % w/v.

[C_4-mim]TFA ionic liquid: pale blue (cooling) and pale red (heating);
[C_4-mim]TFA–[C_{16}-mim]Br solution: bright blue (cooling) and bright red (heating).

TFA = CF_3CO_2

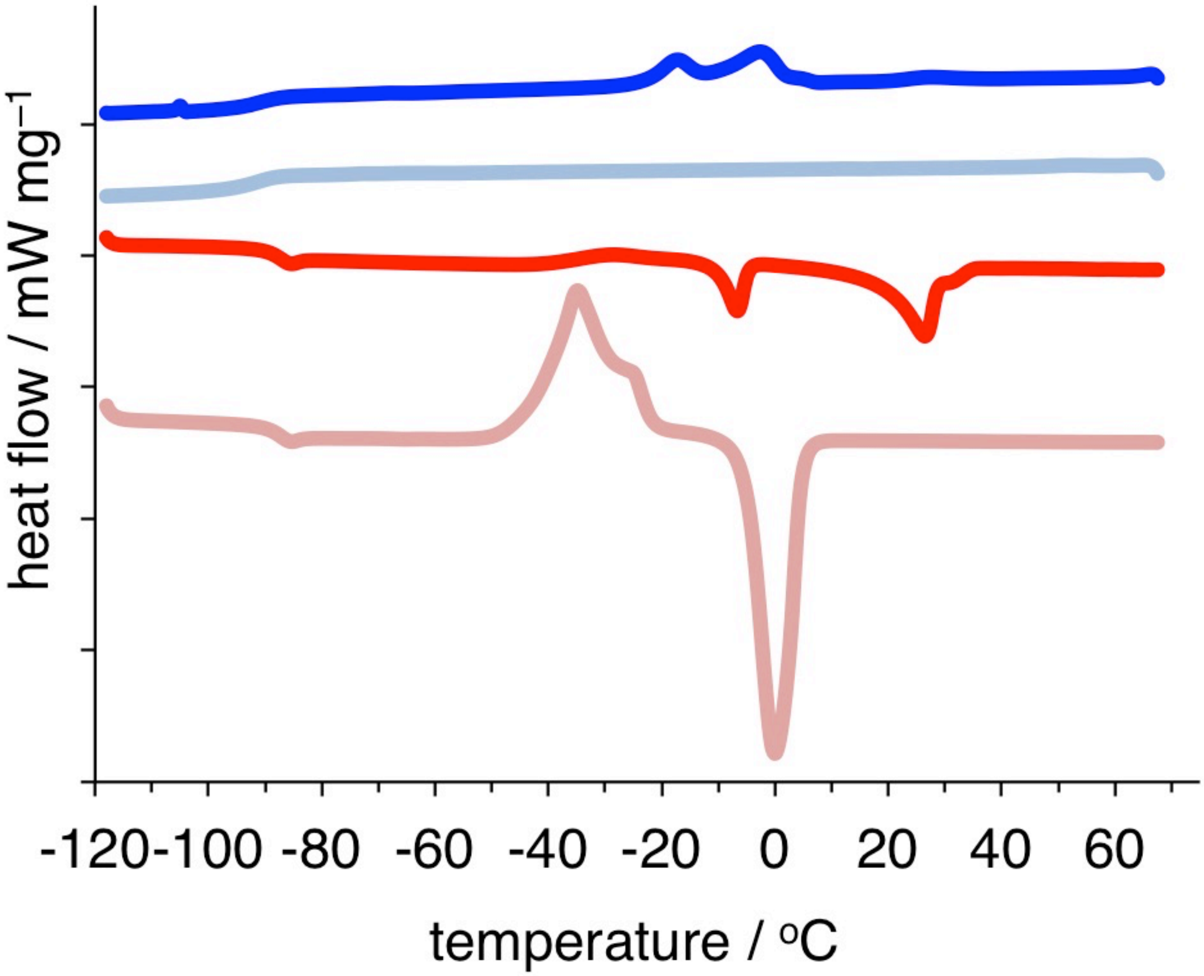

Figure S11. DSC traces of [C_4-mim]NTf_2 and [C_4-mim]NTf_2–[C_{16}-mim]Br solution. Conditions: samples were heated from 25 °C to 70 °C (not shown), cooling from 70 °C to –120 °C (blue traces), heating from –120 °C to 70 °C (red traces). The traces were artificially off-set to demonstrate the differences. [C_{16}-mim]Br concentration was 20.0 % w/v.

[C_4-mim]NTf_2 ionic liquid: pale blue (cooling) and pale red (heating);
[C_4-mim]NTf_2–[C_{16}-mim]Br solution: bright blue (cooling) and bright red (heating).

$NTf_2 = N(SO_2CF_3)_2$

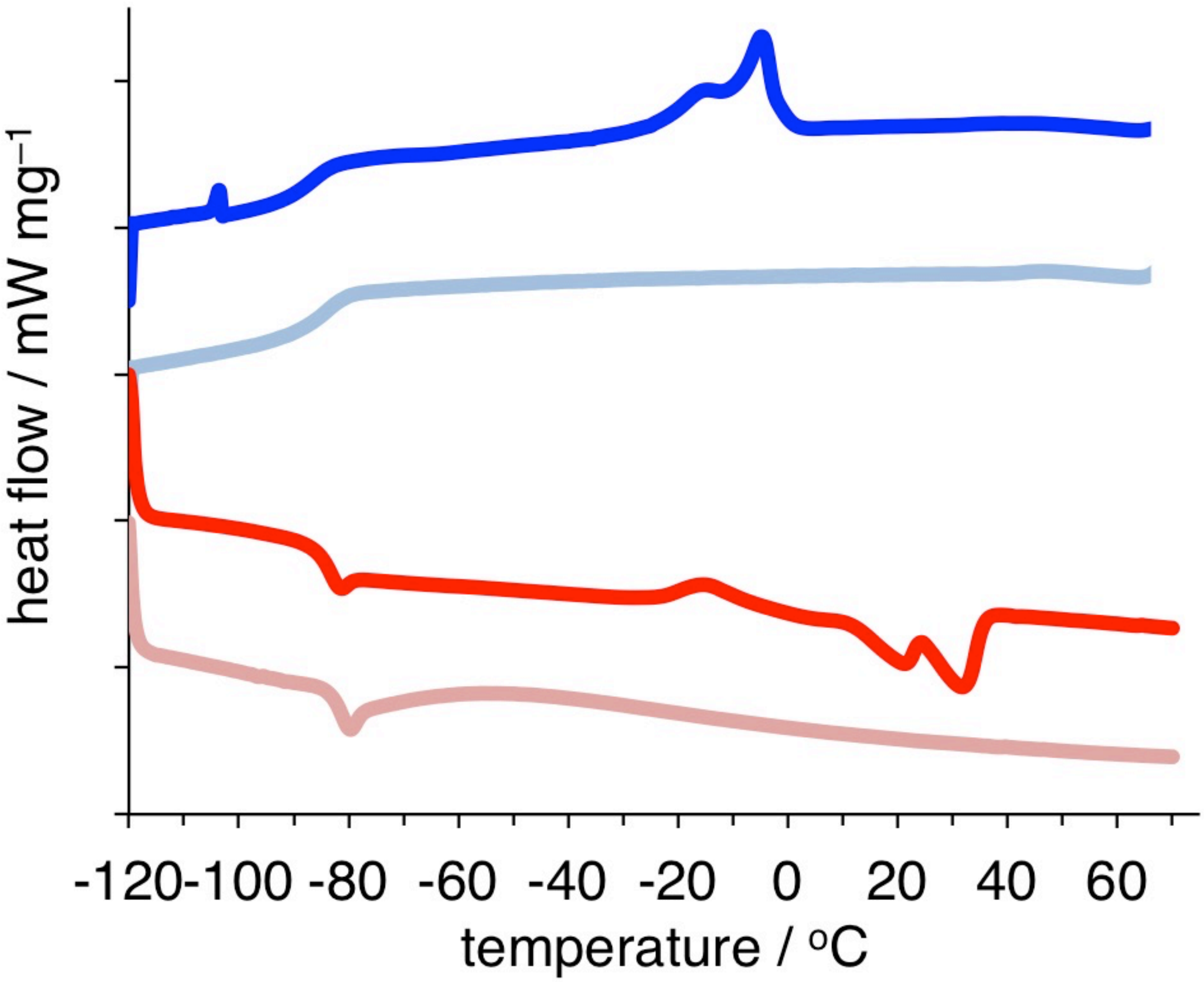

Figure S12. DSC traces of [C_6-mim]NTf_2 and [C_6-mim]NTf_2–[C_{16}-mim]Br solution. Conditions: samples were heated from 25 °C to 70 °C (not shown), cooling from 70 °C to –120 °C (blue traces), heating from –120 °C to 70 °C (red traces). The traces were artificially off-set to demonstrate the differences. [C_{16}-mim]Br concentration was 16.6 % w/v.

[C_6-mim]NTf_2 ionic liquid: pale blue (cooling) and pale red (heating);
[C_6-mim]NTf_2–[C_{16}-mim]Br solution: bright blue (cooling) and bright red (heating).

$NTf_2 = N(SO_2CF_3)_2$

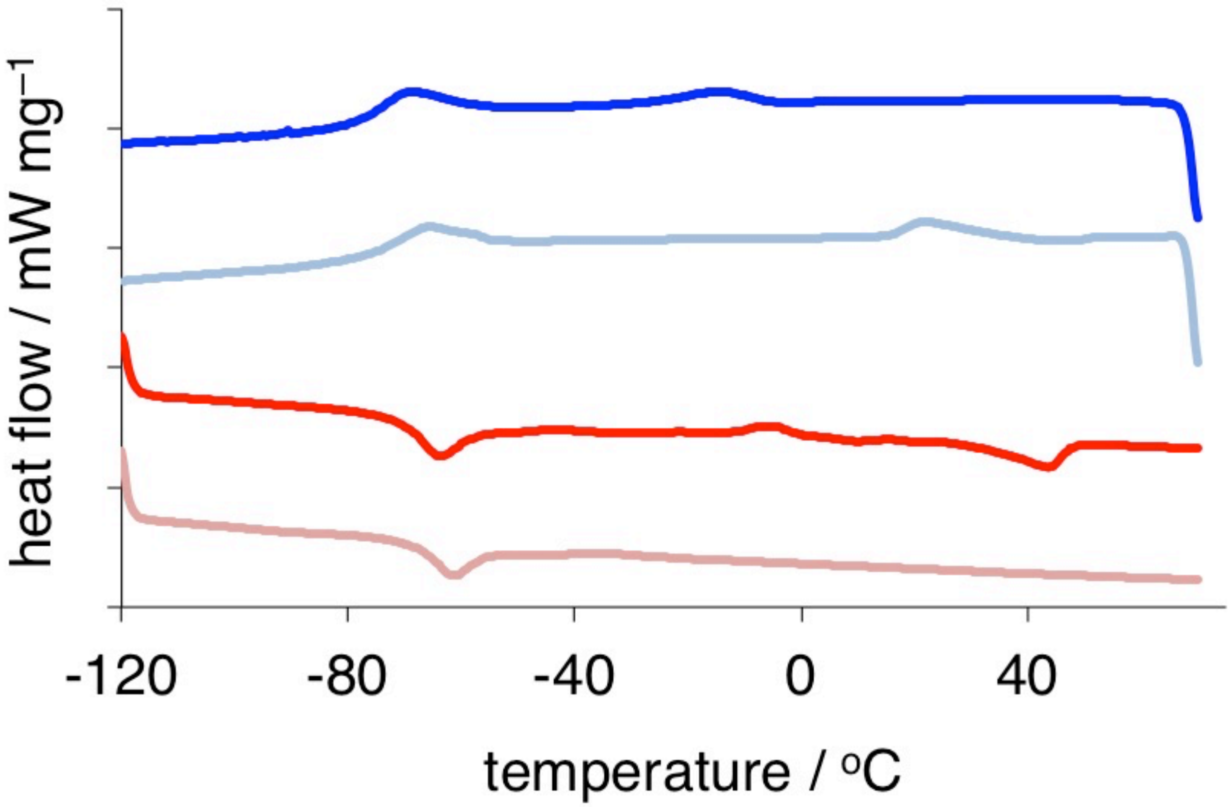

Figure S13. DSC traces of [P_{66614}]Cl and [P_{66614}]Cl–[C_{16}-mim]Br gel.

Conditions: samples were heated from 25 °C to 70 °C (not shown), cooling from 70 °C to –120 °C (blue traces), heating from –120 °C to 70 °C (red traces). The traces were artificially off-set to demonstrate the differences. [C_{16}-mim]Br concentration was 10.0 % w/v.

[P_{66614}]Cl ionic liquid: pale blue (cooling) and pale red (heating);
[P_{66614}]Cl–[C_{16}-mim]Br gel: bright blue (cooling) and bright red (heating).

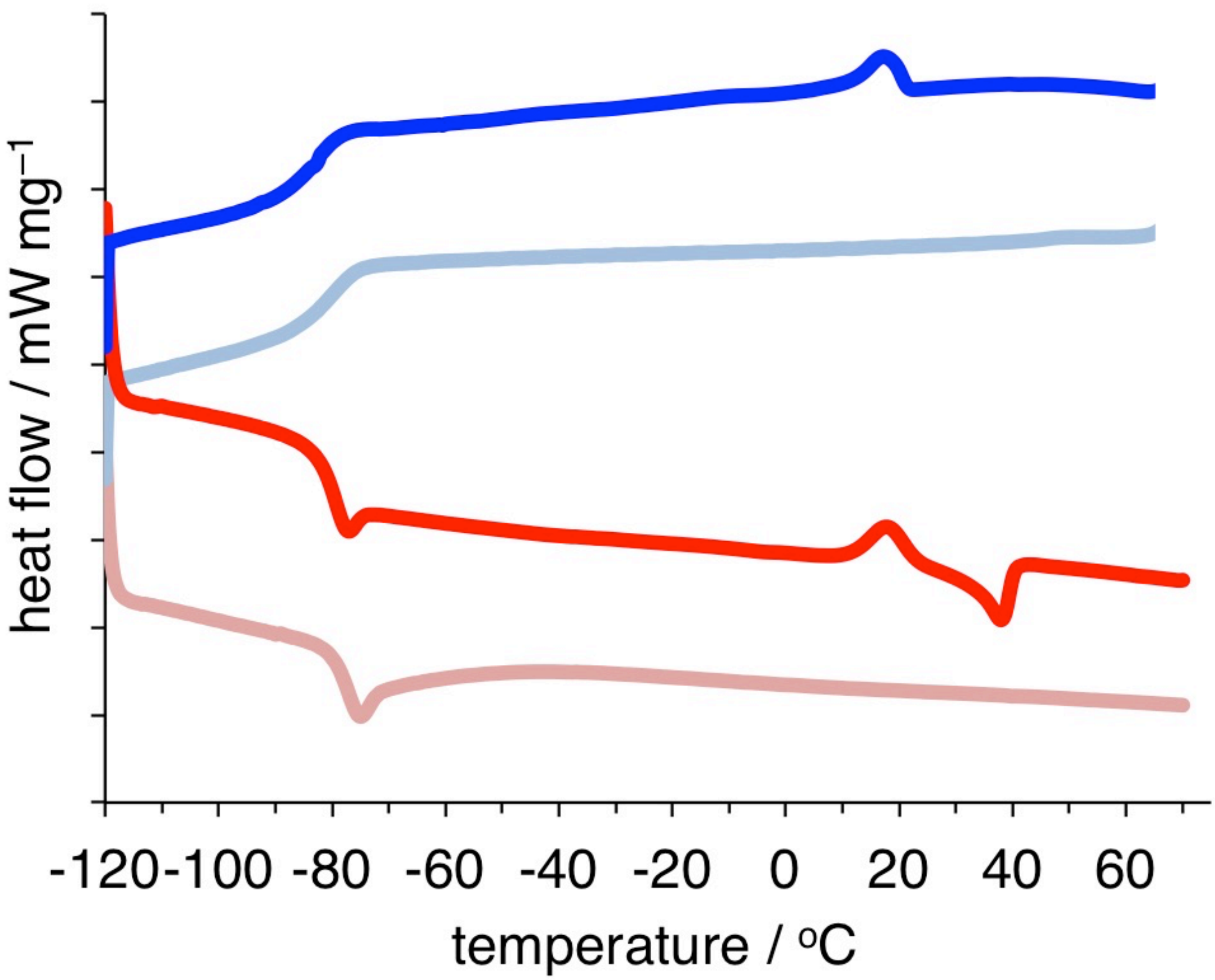

Figure S14. DSC traces of [C_4-py]NO_3 and [C_4-py]NO_3–[C_{16}-mim]Br gel.
Conditions: samples were heated from 25 ^{o}C to 70 ^{o}C (not shown), cooling from 70 ^{o}C to –120 ^{o}C (blue traces), heating from –120 ^{o}C to 70 ^{o}C (red traces). The traces were artificially off-set to demonstrate the differences. [C_{16}-mim]Br concentration was 4.4 % w/v.

[C_4-py]NO_3 ionic liquid: pale blue (cooling) and pale red (heating);
[C_4-py]NO_3–[C_{16}-mim]Br gel: bright blue (cooling) and bright red (heating).

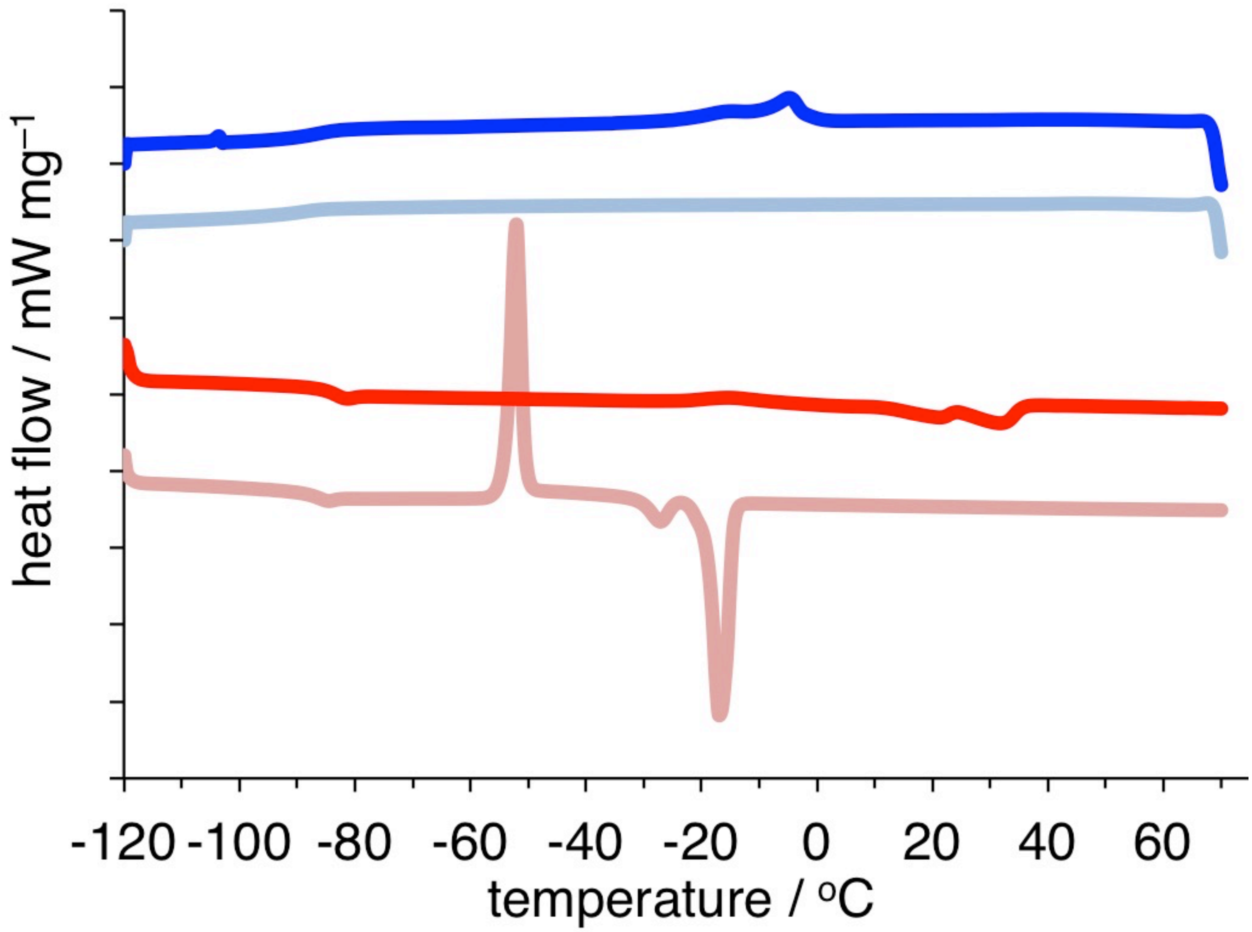

Figure S15. DSC traces of [C_4C_1-pyrr]NTf_2 and [C_4C_1-pyrr]NTf_2–[C_{16}-mim]Br solution. Conditions: samples were heated from 25 °C to 70 °C (not shown), cooling from 70 °C to –120 °C (blue traces), heating from –120 °C to 70 °C (red traces). The traces were artificially off-set to demonstrate the differences. [C_{16}-mim]Br concentration was 24.8 % w/v.

[C_4C_1-pyrr]NTf_2 ionic liquid: pale blue (cooling) and pale red (heating);
[C_4C_1-pyrr]NTf_2–[C_{16}-mim]Br solution: bright blue (cooling) and bright red (heating).

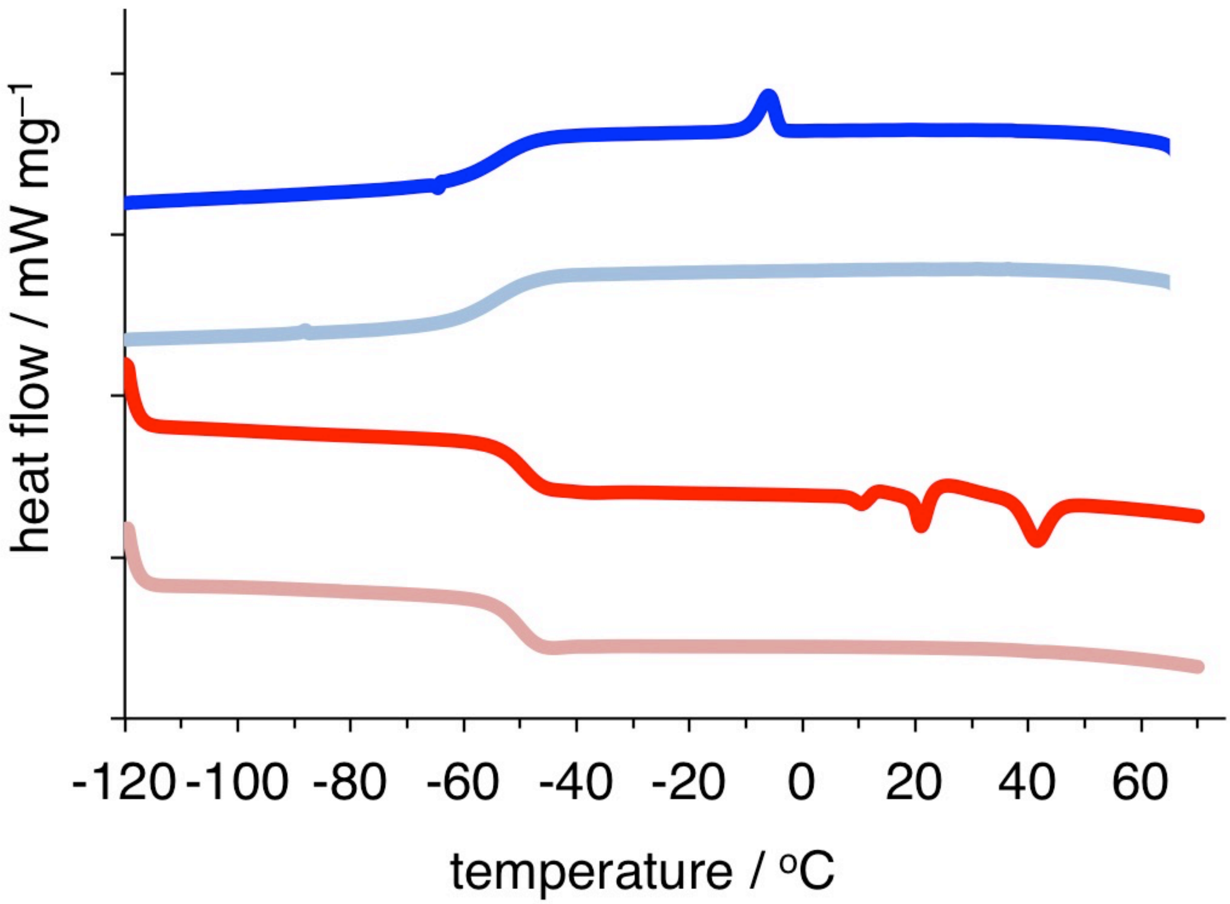

Figure S16. DSC traces of L-Pro/OA and L-Pro/OA–[C_{16}-mim]Br gel.
Conditions: samples were heated from 25 ^{o}C to 70 ^{o}C (not shown), cooling from 70 ^{o}C to –120 ^{o}C (blue traces), heating from –120 ^{o}C to 70 ^{o}C (red traces). The traces were artificially off-set to demonstrate the differences. [C_{16}-mim]Br concentration was 1.0 % w/v.

L-Pro/OA deep-eutectic solvent: pale blue (cooling) and pale red (heating);
L-Pro/OA–[C_{16}-mim]Br gel: bright blue (cooling) and bright red (heating).

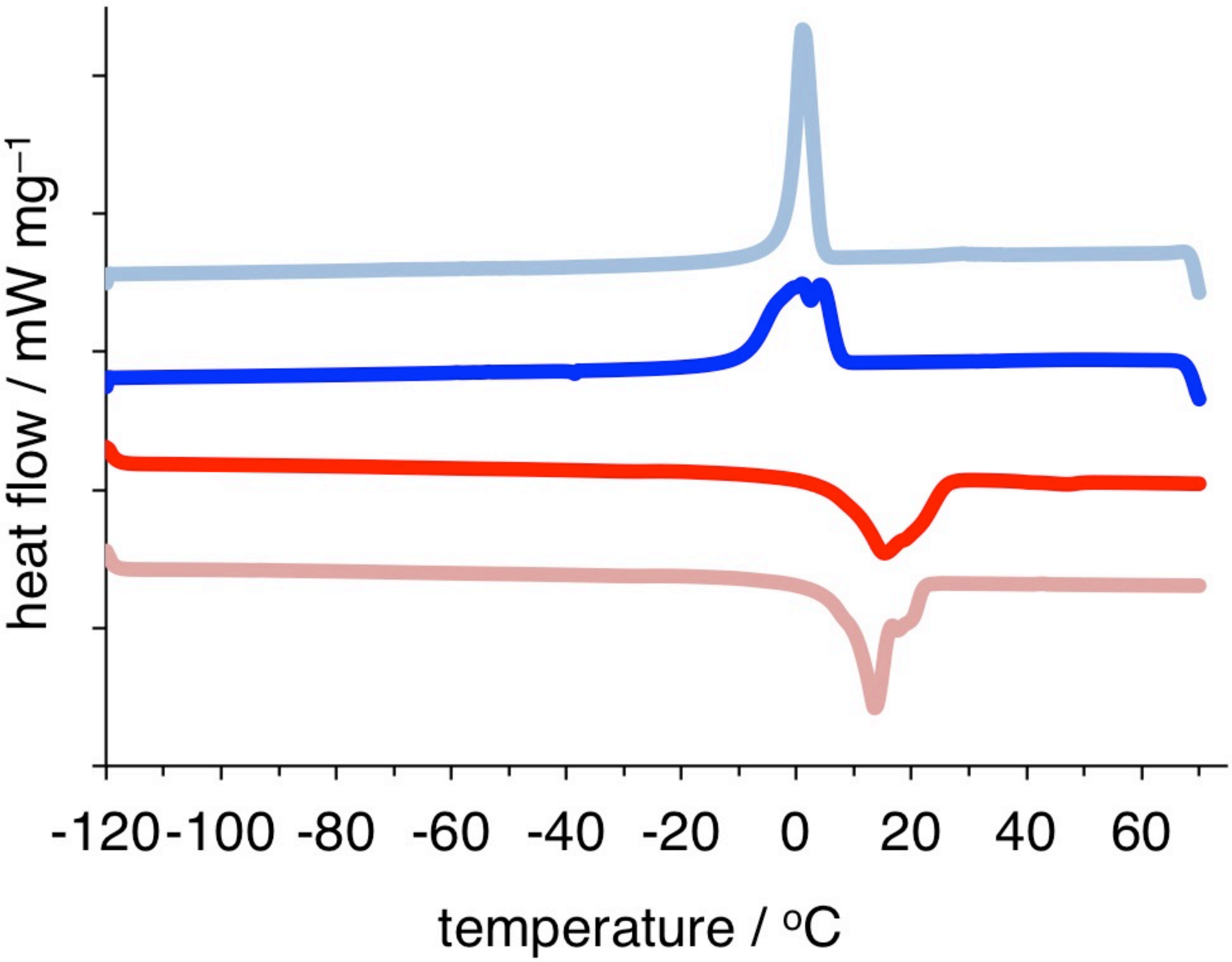

Figure S17. DSC traces of L-menth/$C_{11}H_{23}CO_2H$ and L-menth/$C_{11}H_{23}CO_2H$–[C_{16}-mim]Br gel. Conditions: samples were heated from 25 °C to 70 °C (not shown), cooling from 70 °C to –120 °C (blue traces), heating from –120 °C to 70 °C (red traces). The traces were artificially off-set to demonstrate the differences. [C_{16}-mim]Br concentration was 0.9 % w/v.

L-menth/$C_{11}H_{23}CO_2H$ deep-eutectic solvent: pale blue (cooling) and pale red (heating); L-menth/$C_{11}H_{23}CO_2H$–[C_{16}-mim]Br gel: bright blue (cooling) and bright red (heating).

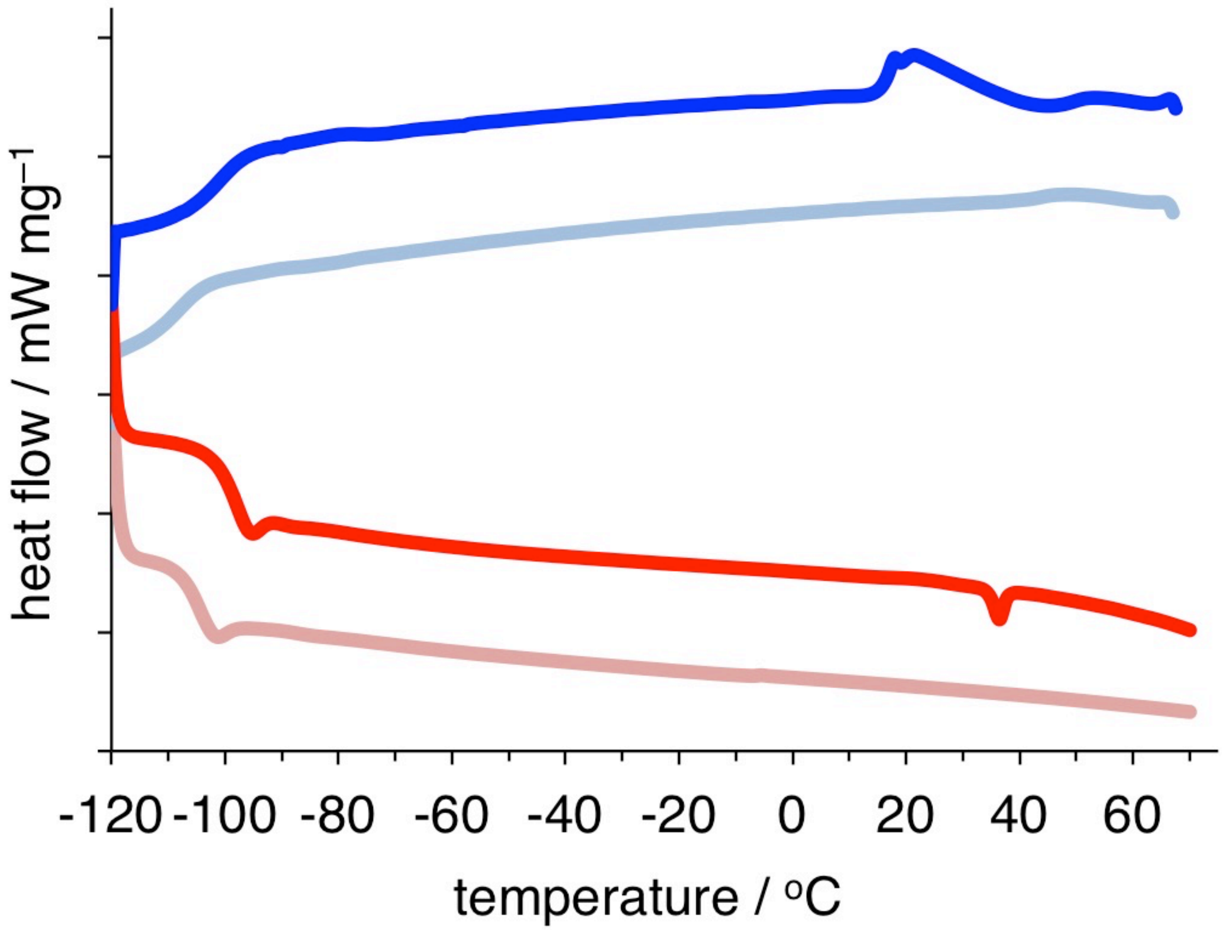

Figure S18. DSC traces of EG/$ZnCl_2$ and EG/$C_{11}H_{23}CO_2H$–[C_{16}-mim]Br gel.
Conditions: samples were heated from 25 ^{o}C to 70 ^{o}C (not shown), cooling from 70 ^{o}C to –120 ^{o}C (blue traces), heating from –120 ^{o}C to 70 ^{o}C (red traces). The traces were artificially off-set to demonstrate the differences. [C_{16}-mim]Br concentration was 1.1 % w/v.

EG/$ZnCl_2$ deep-eutectic solvent: pale blue (cooling) and pale red (heating);
EG/$C_{11}H_{23}CO_2H$–[C_{16}-mim]Br gel: bright blue (cooling) and bright red (heating).

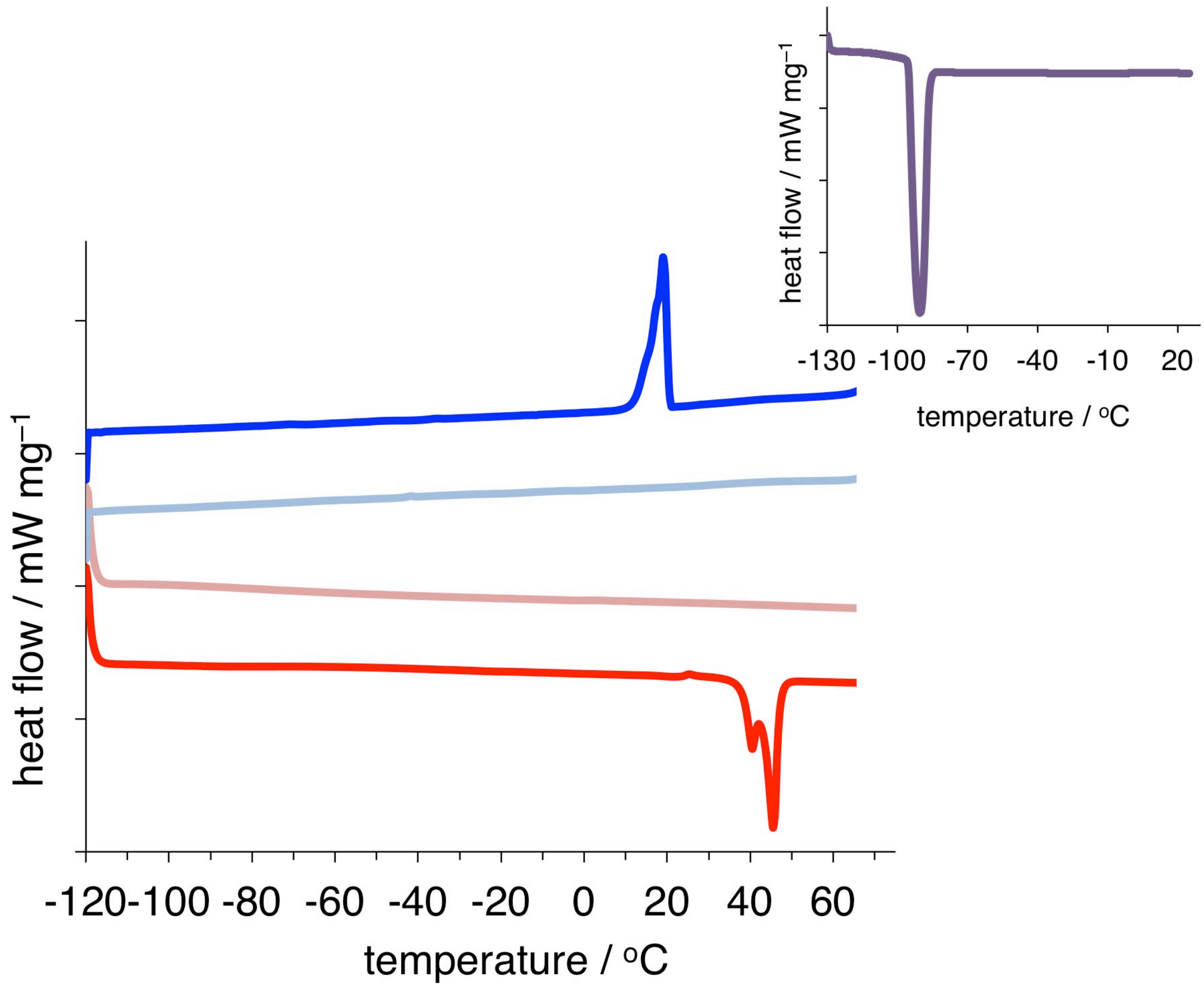

Figure S19. DSC traces of toluene and toluene–[C_{16}-mim]Br gel.
Conditions: samples were heated from 25 °C to 70 °C (not shown), cooling from 70 °C to –120 °C (blue traces), heating from –120 °C to 70 °C (red traces). The traces were artificially off-set to demonstrate the differences. [C_{16}-mim]Br concentration was 9.9 % w/v.

toluene: pale blue (cooling) and pale red (heating);
toluene–[C_{16}-mim]Br gel: bright blue (cooling) and bright red (heating).

Inset: DSC of toluene; conditions: sample cooled to –130 °C (not shown), kept at –130 °C for 20 min (not shown), and heated from –130 to 25 °C (purple trace).

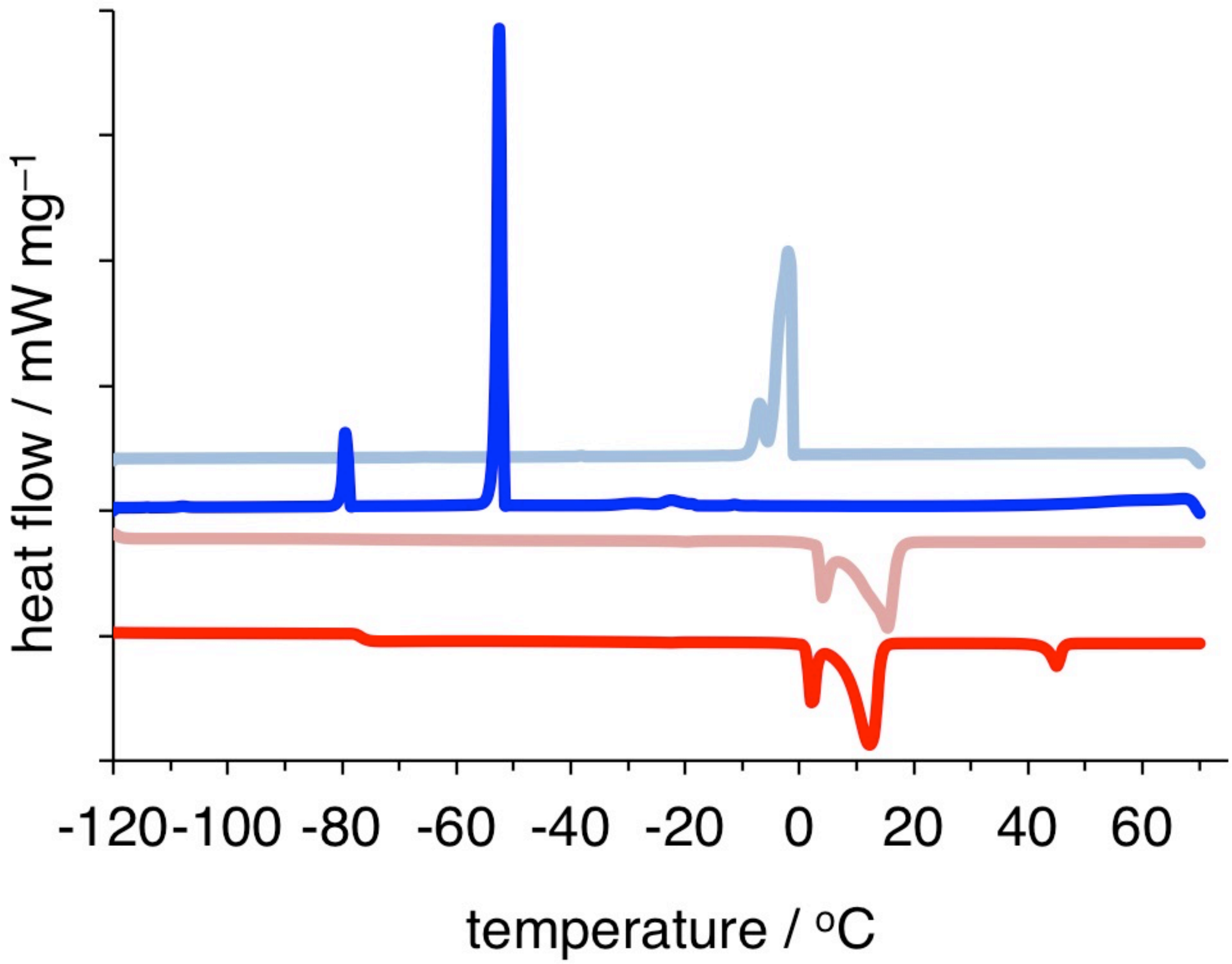

Figure S20. DSC traces of dioxane and dioxane–[C_{16}-mim]Br gel.
Conditions: samples were heated from 25 ^{o}C to 70 ^{o}C (not shown), cooling from 70 ^{o}C to –120 ^{o}C (blue traces), heating from –120 ^{o}C to 70 ^{o}C (red traces). The traces were artificially off-set to demonstrate the differences. [C_{16}-mim]Br concentration was 9.9 % w/v.

dioxane: pale blue (cooling) and pale red (heating);
dioxane–[C_{16}-mim]Br gel: bright blue (cooling) and bright red (heating).

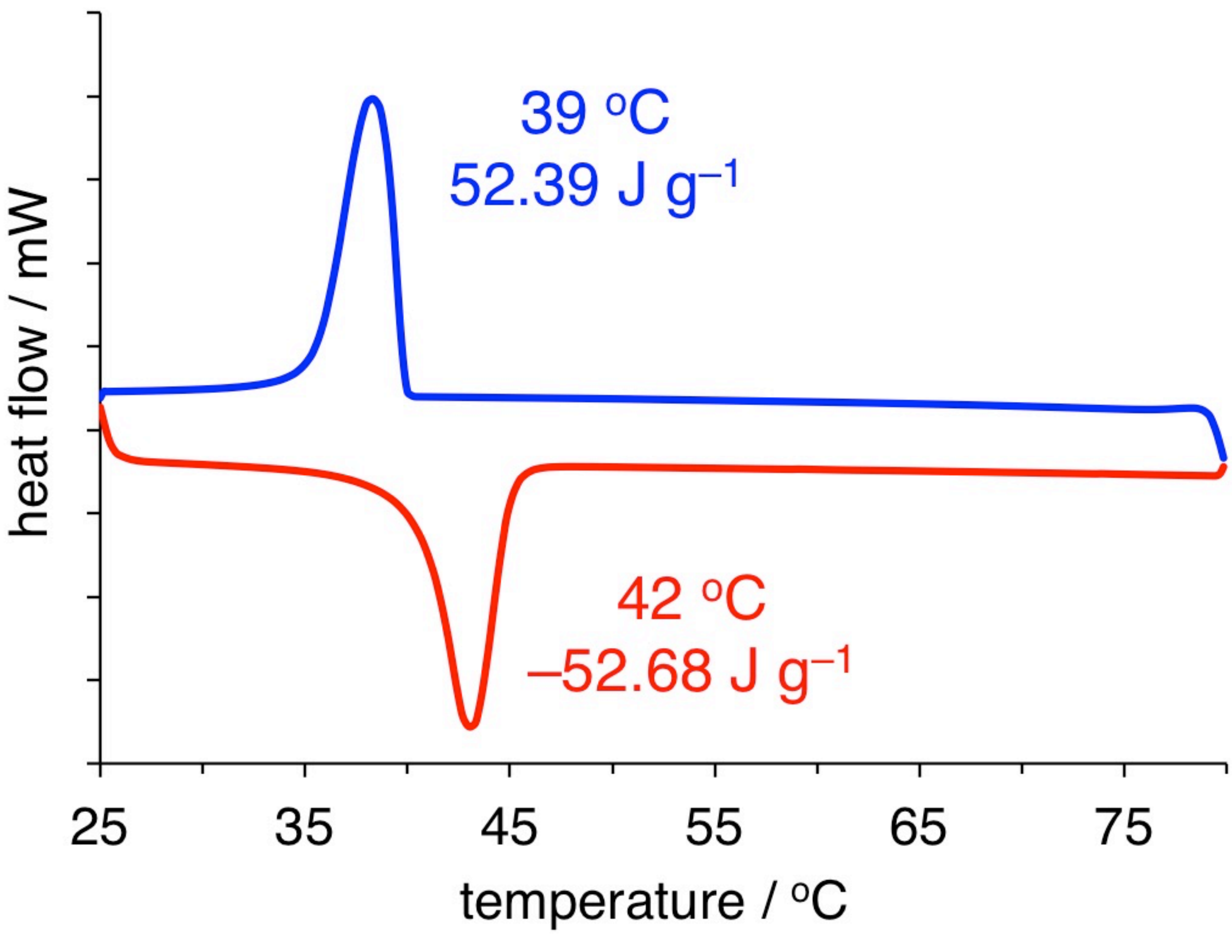

Figure S21. DSC of [C_{16}-mim]Br.

Second heating (red) and cooling (blue) cycles; the corresponding Tc and Tg (reported as the peak's maximum / minimum), with respective ΔH) are given next to the peaks.

The sample was heated from 25 °C to 80 °C and cooled to 25 °C at 10 deg/min in DSC (1st heating/cooling cycle; not shown), and subsequently heated from 25°C to 80 °C (2nd heating cycle) and cooled from 80 °C to 25 °C (2nd cooling cycle). The 3rd heating/cooling cycle (not shown) produced results, which were identical to the 2nd heating/cooling cycle.

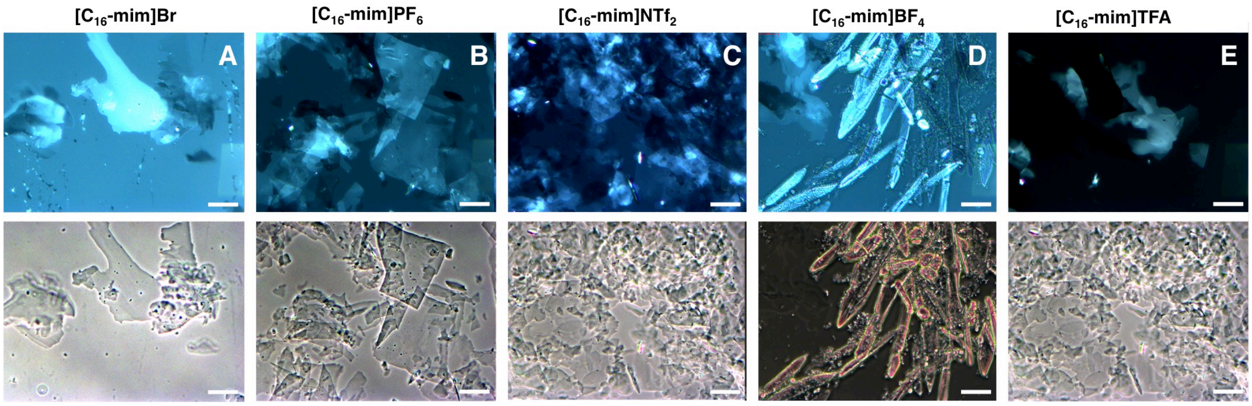

Figure S22. POM images of [C_4-mim]PF_6 gels with different [C_{16}-mim]-gelators. White scale bar is 20 μm.

A: [C_{16}-mim]**Br** (6.0 % w/v);
B: [C_{16}-mim]**PF_6** (5.8 % w/v);
C: [C_{16}-mim]**NTf_2** (3.4 % w/v);
D: [C_{16}-mim]**BF_4** (5.9 % w/v);
E: [C_{16}-mim]**TFA** (5.0 % w/v);
TFA = CF_3CO_2, NTf_2 = $N(SO_2CF_3)_2$.

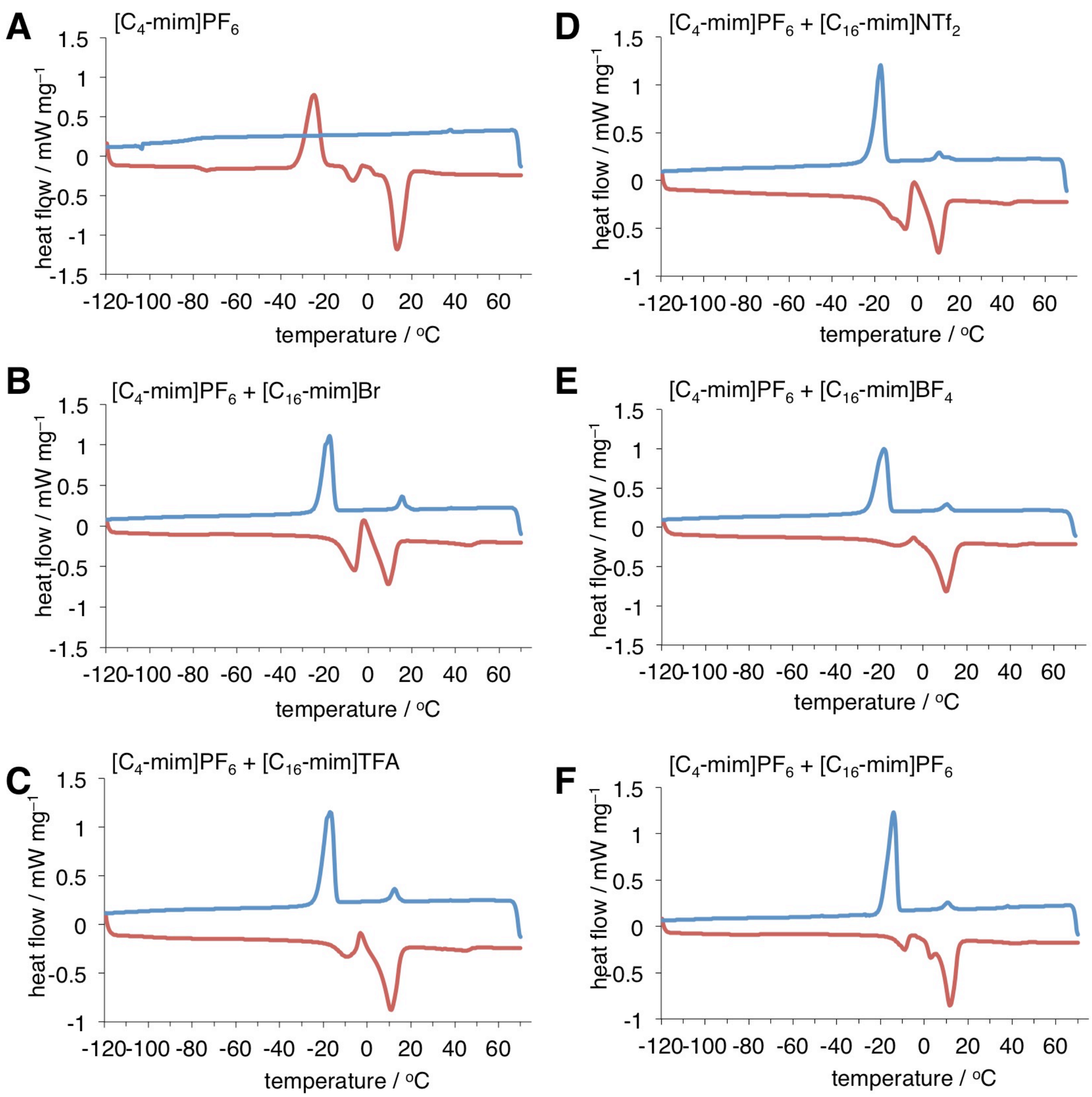

Figure 23. DSC traces of [C_4-mim]PF_6 gels with [C_{16}-mim]X gelators.
Conditions: samples were heated from 25 °C to 70 °C (not shown), cooling from 70 °C to –120 °C (blue trace), heating from –120 °C to 70 °C (red trace).
TFA = CF_3CO_2, NTf_2 = $N(SO_2CF_3)_2$.

A: [C_4-mim]PF_6, no gelator;
B: [C_4-mim]PF_6 and [C_{16}-mim]**Br** (6.0 % w/v);
C: [C_4-mim]PF_6 and [C_{16}-mim]**TFA** (5.0 % w/v);
D: [C_4-mim]PF_6 and [C_{16}-mim]$\mathbf{NTf_2}$ (3.4 % w/v);
E: [C_4-mim]PF_6 and [C_{16}-mim]$\mathbf{BF_4}$ (5.9 % w/v);
F: [C_4-mim]PF_6 and [C_{16}-mim]$\mathbf{PF_6}$ (5.8 % w/v).

Table S1. Phase transitions for ionic liquids and deep-eutectic solvents and their gels as determined from DSC measurements.[a]

entry	system	T_m, °C (ΔH, J g^{-1})[b]	T_c, °C (ΔH, J g^{-1})[b]		T_g, °C (ΔC_P, J g^{-1} K^{-1})[c]
		heating cycle	***cooling cycle***	***heating cycle***	***heating cycle***
	ionic liquids				
1a	[C$_4$-mim]Br				–95 (0.38)
1b	[C$_4$-mim]Br + [C$_{16}$-mim]Br	42 (–3.40)	18 (2.14)	11 (1.95)	–85 (0.47)
2a	[C$_5$-mim]Br				–72 (0.29)
2b	[C$_5$-mim]Br + [C$_{16}$-mim]Br	36 (–3.85)[d]	10 (3.96)		–70 (0.24)
3a	[C$_6$-mim]Br				–74 (0.35)
3b	[C$_6$-mim]Br + [C$_{16}$-mim]Br	38 (–4.26)[d]	–12 (6.41)		–94 (0.43)
4a	[C$_4$-mim]PF$_6$	12 (46.90)[d]		–26 (39.69)	–79 (0.29)
4b	[C$_4$-mim]PF$_6$ + [C$_{16}$-mim]Br	9 (–33.51)[d] 46 (–2.45)	16 (3.38) –17 (30.70)		
5a	[C$_6$-mim]PF$_6$				–74 (0.31)
5b	[C$_6$-mim]PF$_6$ + [C$_{16}$-mim]Br	27 (–1.96)	–9 (2.80)		–76 (0.39)
6a	[C$_4$-mim]NO$_3$	–1 (–0.71)			–97 (0.49)
6b	[C$_4$-mim]NO$_3$ + [C$_{16}$-mim]Br	–2 (0.29) 27 (–4.84)	22 (4.29)[d]		–98 (0.42)
7a	[C$_6$-mim]NO$_3$	–75 (5.86)			
7b	[C$_6$-mim]NO$_3$ + [C$_{16}$-mim]Br	16 (–12.47)[d]	3 (10.68)[d]		–94 (0.75)
8a	[C$_4$-mim]BF$_4$				–77 (0.30)
8b	[C$_4$-mim]BF$_4$ + [C$_{16}$-mim]Br	25 (–2.60)[d]	16 (3.25)		–76 (0.30)
9a	[C$_4$-mim]TFA				–93 (0.43)
9b	[C$_4$-mim]TFA + [C$_{16}$-mim]Br	30 (–20.43)[d]	17 (10.89) –1 (9.70)		–97 (0.32)
10a	[C$_4$-mim]NTf$_2$			–35 (41.67)[d] –1 (–48.83)	–88 (0.27)
10b	[C$_4$-mim]NTf$_2$ + [C$_{16}$-mim]Br	–7 (–0.04)[d] 26 (–14.49)[d]	27 (0.67) –3 (12.08)[d]		–89 (0.26)
11a	[C$_6$-mim]NTf$_2$	–80 (–3.44)			
11b	[C$_6$-mim]NTf$_2$ + [C$_{16}$-mim]Br	31 (–6.96)[d]	–5 (8.78)[d]	–16 (2.59)	–85 (0.28)
12a	[P$_{66614}$]Cl	–62 (–10.08)	22 (4.18) –65 (10.28)		
12b	[P$_{66614}$]Cl + [C$_{16}$-mim]Br	–63 (–12.26) 43 (–6.78)	–14 (4.39) –69 (11.83)	–5 (1.66)[d]	

entry	system	T_m, °C (ΔH, J g^{-1})[b]	T_c, °C (ΔH, J g^{-1})[b]		T_g, °C (ΔC_P, J g^{-1} K^{-1})[c]
		heating cycle	*cooling cycle*	*heating cycle*	*heating cycle*
13a	[C_4-py]NO_3	–75 (6.93)			
13b	[C_4-py]NO_3 + [C_{16}-mim]Br	38 (–1.71)	17 (1.71)	18 (2.10)	–81 (0.44)
14a	[C_4C_1-pyrr]NTf_2	–27 (–2.84) –17 (25.67)		–52 (22.47)	–88 (0.25)
14b	[C_4C_1-pyrr]NTf_2 + [C_{16}-mim]Br	–9 (–38.17) 33 (–10. 16)	1 (7.58)	–38 (31.17)	–87 (0.24)
	deep-eutectic solvents				
15a	L-Pro/OA				–51 (0.95)
15b	L-Pro/OA + [C_{16}-mim]Br	41 (–1.14)[d]	–6 (2.42)		–50 (0.88)
16a	L-menth/$C_{11}H_{23}CO_2H$	13 (–83.00)[d]	2 (81.11)		
16b	L-menth/$C_{11}H_{23}CO_2H$ + [C_{16}-mim]Br	14 (–84.17)[d] 46 (–1.64)	2 (82.75)[d]		
17a	EG/$ZnCl_2$				–88 (0.28)
17b	EG/$ZnCl_2$ + [C_{16}-mim]Br	43 (–0.58)		21 (0.82)	–104 (0.60)
	molecular solvents				
18a	toluene[e]	–91 (–60.16)			
18b	toluene + [C_{16}-mim]Br	45 (–14.56)[d]	20 (13.57)[d]		
19a	dioxane	13 (–151.98)[d]	2 (149.09)[d]		
19b	dioxane + [C_{16}-mim]Br	12 (–143.73)[d] 45 (–12.60)	–22 (8.81) –50 (121.53) –79 (19.89)		–77 (1.88)

[a] – see Table 1 for minimum [C_{16}-mim]Br gelator concentration and m.p. values; Conditions (unless otherwise noted): samples were heated from 25 °C to 70 °C (the cycle is not reported), *cooling cycle*: from 70 °C to –120 °C, *heating cycle*: from –120 °C to 70 °C. ΔH and ΔC_p values are referred to the amount (in g) of the total sample (fluid + gelator). Heating/cooling rates: 10 deg/min;

[b] – temperature value at the peak maximum/minimum is reported;

[c] – T_g are reported using the heating cycle (–120 to 70 °C) only as the midpoint of the glass transition, due to a better quality of the baseline achieved during the heating cycle;

[d] – multiple overlapping transitions; overall integral is reported; T_m or T_c refers to the peak's maximum/minimum;

[e] – conditions: sample was cooled to –130 °C, kept at –130 °C for 20 min, then heated to 25 °C at 10 deg/min. No phase transitions were observed under conditions given in [a].

Table S2. Effect of the gelator's anion on the gelation of [C_4-mim]PF_6.[a]

entry	[C_{16}-mim]X	MGC, % w/v (m.p. ^oC)
	X	
1	Br	6.0 (41)
2	BF_4	5.0 (34)
3	PF_6	3.4 (36)
4	TFA	5.9 (39)
5	NTf_2	5.8 (39)

[a] – MGC: minimum gelator concentration; melting points determined using the inverted vial method; TFA = CF_3CO_2, NTf_2 = $N(SO_2CF_3)_2$.

Table S3. Effect of the cation on the gelation of various liquids.[a]

gelator	MGC, % w/v (m.p. / ^oC)					
	[C_4-mim]PF_6	**[P_{66614}]Cl**	**EG/$ZnCl_2$**	**L-ment/$C_{11}H_{23}CO_2H$**	**toluene**	**dioxane**
[C_{16}-mim]Br	6.0 (41)	10.0 (37)	1.1 (38)	0.9 (41)	9.9 (35)	9.9 (41)
[C_{16}-py]Br	2.9 (43)	8.7 (48)	4.0 (35)	2.5 (46)	–[b]	8.0 (29)
[$C_{16}C_1$-pyrr]Br	5.9 (33)	9.9 (38)	10.0 (28)	9.1 (34)	–[b]	15.0 (35)

[a] – MGC: minimum gelator concentration; melting points determined using the inverted vial method. [b] – no gelation upon addition of 15.0 % w/v of the gelator.

References

1. Dzyuba, S. V.; Bartsch, R. A. Efficient synthesis of 1-alkyl(aralkyl)-3-methyl(ethyl)imidazolium halides: precursors for room-temperature ionic liquids. *J. Heterocyclic Chem.* **2001**, *38*, 265–268.
2. Dzyuba, S. V.; Bartsch, R. A. Influence of structural variations in 1-alkyl(aralkyl)-3-methylimidazolium hexafluorophoshates and bis(trifluoromethylsulfonyl)imides on physical properties of the ionic liquids. *ChemPhysChem* **2002**, *3*, 161–166.
3. Smith, N. W.; Gourisankar, S. P.; Montchamp, J.-L.; Dzyuba, S. V. Silver-free synthesis of nitrate-containing room-temperature ionic liquids. *New J. Chem.* **2011**, *35*, 909–914.
4. Holbrey, J. D.; Seddon, K. R. *J.* The Phase behavior of 1-alkyl-3-methylimidazolium tetrafluoroborates; ionic liquid and ionic liquid crystals. *Chem. Soc., Dalton Trans.* **1999**, 2133–2140.
5. Jameson, L. P.; Dzyuba, S. V. Ionic liquid-controlled conformational bias of tetracycline. *RSC Adv*. **2013**, *3*, 4582–4587.
6. Kakinuma, S.; Shirota, H. Femtosecond Raman-induced Kerr effect study of temperature dependent intermolecular dynamics in molten bis(trifluoromethylsulfonyl)amide salts: effect of cation species. *J. Phys. Chem. B* **2018**, *122*, 6033–6047.
7. Du, M.; Dai, C.; Chen, A.; Wu, X.; Li, Y.; Liu, Y.; Li, W.; Zhao, M. Investigation of the aggregation behavior of photo-responsive system composed of 1-hexadecyl-3-methylimidazolium bromide and 2-methoxycinnamic acid. *RSC Adv.* **2015**, *5*, 68369–68377.
8. Gordon, C. M.; Holbrey, J. D.; Kennedy, A. R.; Seddon, K. R. Ionic liquid crystals: hexafluorophosphate salts. *J. Mater. Chem.* **1998**, *8*, 2627–2636.
9. Paulechka, E.; Blokhin, A. V.; Rodrigues, A. S. M. C.; Rocha, M. A. A.; Luis, L. M. N. B. F. Thermodynamics of long-chain 1-alkyl-3-methylimidazolium bis(trifluoromethanesulfonyl)imide ionic liquids. *J. Chem. Thermodynamics* **2016**, *97*, 331–340.
10. Marek, J.; Stodulka, P.; Cabal, J.; Soukup, O.; Pohanka, M.; Korabecny, J.; Musilek, K.; Kuca, K. Preparation of the pyridinium salts differing in the length of the N-alkyl substituent. *Molecules* **2010**, *15*, 1967–1972.
11. Goossens, K.; Lava, K.; Nockermann, P.; Van Henke, K.; Van Meervelt, L.; Driesen, K.; Gorller-Walrand, C.; Binnemans, K.; Cardinaels, T. Pyrrolidinium ionic liquid crystals. *Chem. Eur. J.* **2009**, *15*, 656–674.